JOURNAL OF PETROLOGY

Journal of Petrology, 2015, Vol. 56, No. 7, 1343–1364
doi: 10.1093/petrology/egv039
Advance Access Publication Date: 12 August 2015
Original Article

OXFORD

The Transition from Agpaitic to Hyperagpaitic Magmatic Crystallization in the Ilímaussaq Alkaline Complex, South Greenland

Tom Andersen[1]* and Henrik Friis[2]

[1]Department of Geosciences, University of Oslo, PO Box 1047 Blindern, N-0316 Oslo, Norway and [2]Natural History Museum, University of Oslo, PO Box 1172 Blindern, N-0318 Oslo, Norway

*Corresponding author. E-mail: tom.andersen@geo.uio.no

Received October 16, 2014; Accepted June 26, 2015

ABSTRACT

Hyperagpaitic rocks are highly peralkaline nepheline syenites in which minerals such as ussingite [$Na_2AlSi_2O_8(OH)$] and naujakasite ($Na_6FeAl_4Si_8O_{26}$) crystallize instead of, or in addition to, feldspars and feldspathoids; eudialyte is succeeded by steenstrupine-(Ce) and members of the lovozerite and lomonosovite groups; highly water-soluble minerals such as villiaumite (NaF) and natrosilite ($Na_2Si_2O_5$) form part of magmatic mineral assemblages. Hyperagpaitic magmatic rocks in the Ilímaussaq alkaline complex in South Greenland include intrusive bodies of villiaumite- and naujakasite-bearing lujavrite (i.e. melanocratic, silica-undersaturated syenite), and late veins and pegmatites. The transition from agpaitic to hyperagpaitic magmatic conditions is controlled by increasing peralkalinity (or $a_{Na2Si2O5}$) and changes in activities of water, halogens and phosphorus. The relative importance of these parameters can be evaluated by chemographic analysis based on observed mineral assemblages and mineral compositions. Highly peralkaline melts can crystallize agpaitic albite + microcline + nepheline + arfvedsonite + eudialyte ± sodalite magmatic assemblages over a wide range of alkali, water and halogen activities. In most cases, a net increase in HF activity is needed to induce villiaumite crystallization, suggesting hyperagpaitic conditions, but because of the orientation of the villiaumite-saturation surface in log $a_{Na2Si2O5}$–log a_{H2O}–log a_{HF} space, loss of an aqueous fluid may stabilize villiaumite without increasing peralkalinity. Naujakasite indicates elevated $a_{Na2Si2O5}$, ussingite elevated a_{H2O}, and steenstrupine-(Ce) and vuonnemite high $a_{Na2Si2O5}$ and a_{P2O5}. Closed-system fractionation of agpaitic magma may lead to hyperagpaitic residual liquids if aegirine, eudialyte or sodalite do not crystallize early, which is not applicable to the main line of magma evolution in Ilímaussaq, with abundantly eudialyte-bearing kakortokite and sodalite-bearing naujaite cumulates. Hyperagpaitic residual liquids can have developed if fractionation of these minerals were suppressed, or by open-system processes such as intraplutonic assimilation of sodalite-bearing cumulates in lujavritic magma at low a_{HCl}.

Key words: agpaitic rocks; hyperagpaitic rocks; Ilímaussaq complex; naujakasite; ussingite; villiaumite

INTRODUCTION

Agpaitic rocks are highly peralkaline nepheline syenites in which zirconium, titanium and other high field strength elements (HFSE) are hosted in volatile- and alkali-bearing silicate minerals rather than in zircon, ilmenite and titanite, which host HFSE in miaskitic rocks (e.g. Sørensen, 1997, and references therein). Agpaitic rocks are found as major intrusive members of a few large plutons (e.g. Khibina, Lovozero, Ilímaussaq; Sørensen, 1974), and as minor components in otherwise non-agpaitic alkaline rock complexes (e.g. Oslo Rift: Larsen, 2010; Tamazeght: Salvi *et al.*, 2000; Schilling *et al.*, 2009). Elements such as Zr, Nb, Y, rare earth elements (REE), Th and U are commonly enriched

in agpaitic rocks, in some cases reaching ore grade (Sørensen, 1992; Chakmouradian & Zaitsev, 2012, and references therein). In hyperagpaitic rocks, the evolution away from ordinary, igneous mineralogy has gone one step further: exotic minerals such as ussingite and naujakasite (see Table 1 for mineral formulae) take the place of feldspar and feldspathoids; complex phosphosilicate minerals such as steenstrupine-(Ce) and lomonosovite, or highly alkaline members of the lovozerite group, replace eudialyte; and vuonnemite and minerals that are water soluble or otherwise unstable at surface conditions crystallize (e.g. villiaumite, natrosilite; e.g. Khomyakov, 1995; Sørensen & Larsen, 2001). More than 40 water-soluble minerals have been described from hyperagpaitic rocks in the Khibina and Lovozero complexes, Kola Peninsula (Khomyakov, 1995). In Ilímaussaq, SW Greenland, fewer have been found; for example, trona and thermonatrite (Sørensen *et al.*, 1970), dorfmanite (Petersen *et al.*, 1993), natrophosphate (Petersen *et al.*, 2001) and abundant villiaumite. E. Sørensen (1982) suggested that other water-soluble minerals should be present in Ilímaussaq, especially natrosilite, which has now been identified (H. Friis, unpublished data). The apparent scarcity of water-soluble minerals in Ilímaussaq, compared with the Kola complexes, is not because Ilímaussaq is less hyperagpaitic but is a result of extensive mining in Kola, which exposes unaltered rocks and hence preserved water-soluble minerals. The water-soluble minerals have an inverse solubility with temperature, which explains how they can be primary and form even in water-rich fluids (Kogarko, 1977).

Hyperagpaitic rocks are commonly late, minor members of agpaitic nepheline syenite complexes, and can in most cases be accounted for by the effects of highly alkaline, late-magmatic or post-magmatic fluids on less alkaline igneous rocks within the plutons (Khomyakov, 1995). In the Ilímaussaq complex, hyperagpaitic pegmatites, veins and alteration zones are common (Danø & Sørensen, 1959; Bondam & Ferguson, 1962; Markl & Baumgartner, 2002), but, in addition, hyperagpaitic naujakasite-, steenstrupine-(Ce)- and villiaumite-bearing lujavrite form intrusive bodies of considerable size (Khomyakov *et al.*, 2001; Sørensen & Larsen, 2001; Rose-Hansen & Sørensen, 2002; Sørensen *et al.*, 2011). Potentially economic U, Th and REE mineralization is hosted in hyperagpaitic lujavrite and associated rocks (Sørensen *et al.*, 2011).

Since the pioneering work of Ussing (1912), it has been generally agreed that the main reason why agpaitic mineral assemblages form in some nepheline syenites is extreme peralkalinity, expressed by a (Na + K)/Al ratio (agpaitic index or *AI*) far above unity; according to Ussing's original definition, an agpaitic rock should have $AI > 1{\cdot}2$. However, because volatile-bearing minerals are ubiquitous in agpaitic rocks, the activities of volatile components (water, halogens) must also be important for the evolution of agpaitic magmas; Brøgger (1890) pointed this out well before the concept of agpaitic rocks had been introduced. Recent studies on the mildly agpaitic nepheline syenite pegmatites in the Oslo Rift, Norway have shown that, although increasing peralkalinity is the main driving force behind the transition from miaskitic (i.e. zircon stable) to agpaitic crystallization conditions, the activities of water, fluorine (or HF) and chlorine (or HCl) control the magmatic mineralogy of a nepheline syenite magma, and will under certain conditions cause a shift to agpaitic mineralogy without a concomitant increase in peralkalinity (Andersen *et al.*, 2010, 2013).

The transition from the agpaitic to the hyperagpaitic realm involves a change in stable volatile-bearing mineralogy. For example, whereas fluorite is found as a minor mineral in the agpaitic rocks, villiaumite (NaF) is abundant in the hyperagpaitic rocks. Eudialyte (with Cl) is unstable in hyperagpaitic naujakasite lujavrite; instead, steenstrupine-(Ce) with water and phosphorus but no chlorine is the most abundant Zr-bearing mineral (Khomyakov, 1995). An influence of water and halogens on the transition process may be assumed (Sørensen & Larsen, 2001), but the relative effects of volatile components and peralkalinity remain unknown. The importance of these parameters can be deduced from chemographic analysis of magmatic mineral assemblages (Andersen & Sørensen, 2005; Andersen *et al.*, 2010, 2013; Marks *et al.*, 2011). The current study applies this approach to explore the transition from an agpaitic to a hyperagpaitic crystallization regime in highly peralkaline nepheline syenite magma. The study is largely based on our own observations and published petrographic data and mineral analyses from the Ilímaussaq intrusion in South Greenland, but the mineralogical similarity to other agpaitic to hyperagpaitic systems (e.g. in the Lovozero and Khibina intrusions in Russia, Mont Saint-Hilaire in Canada) makes the findings applicable to similar rocks elsewhere.

GEOLOGICAL SETTING

The Ilímaussaq intrusion (Sørensen, 2001; Upton, 2014; Marks & Markl, 2015) is an alkaline layered intrusion belonging to the late period of evolution in the Gardar Rift (*c.* 1160 Ma; Waight *et al.*, 2002; Krumrei *et al.*, 2006). It was emplaced into Palaeoproterozoic granitic basement, with overlying sandstones and lavas, and into older Gardar intrusions (Ussing, 1912; Allaart, 1973). The exposed part of the intrusion (see simplified sketch in Fig. 1) is made up by an outer shell consisting of a border group of non-agpaitic augite syenite and agpaitic pegmatites, and an upper border group with augite syenite, pulaskite, alkali syenite and alkali granite, and a larger, central part of various agpaitic rocks. The agpaitic rocks include an upper series of mildly agpaitic sodalite foyaite and strongly agpaitic naujaite (i.e. sodalite-rich nepheline syenite) roof cumulates, and a floor series of kakortokite (i.e. modally layered arfvedsonite, eudialyte and nepheline + alkali feldspar cumulates). Different varieties of aegirine and

Table 1: Mineral compositions relevant for the agpaitic to hyperagpaitic transition

Mineral	Abbreviation	Formula used in model calculations	Reference
Albite	Ab	$NaAlSi_3O_8$	Ideal composition
Nepheline	Ne	$KNa_3(AlSiO_4)_4$	Model composition
Microcline	Mc	$KAlSi_3O_8$	Ideal composition
Analcime	Anl	$NaAlSi_2O_6{\cdot}H_2O$	Ideal composition
Natrolite	Nat	$Na_2Al_2Si_3O_{10}{\cdot}2H_2O$	Ideal composition
Arfvedsonite	Arf	$Na_3Fe^{III}Fe^{II}_4Si_8O_{22}(OH)_2$	Ideal composition
Ussingite	Uss	$Na_2AlSi_3O_8(OH)$	Ideal composition
Naujakasite	Naj	$Na_6FeAl_4Si_8O_{26}$	Ideal composition
Polylithionite	Plt	$KLi_2AlSi_4O_{10}(F,OH)_2$	Ideal composition
Natrosilite	Nsl	$Na_2Si_2O_5$	Ideal composition
Fluorite	Flu	CaF_2	Ideal composition
Villiaumite	Vil	NaF	Ideal composition
Hiortdahlite	Hio	$Na_{1.81}Ca_{4.52}Fe_{0.25}RE_{0.09}Zr_{1.13}Ti_{0.09}Nb_{0.12}Si_4O_{28}F_{3.45}O_{0.55}$	Robles *et al.* (2001)
Catapleiite	Cat	$Na_{1.4}Ca_{0.3}ZrSi_3O_9{\cdot}2H_2O$	Model composition
Zircon	Zrc	$ZrSiO_4$	Ideal composition
Eudialyte	Eud	$Na_{14.66}K_{0.17}Ca_{5.39}(Mn,Fe)_{3.08}REE_{0.15}Zr_{2.70}Ti_{0.02}Nb_{0.21}Al_{0.15}Si_{26.12}O_{75.71}(OH)_2Cl_{1.33}$	Pfaff *et al.* (2008)
Voronkovite*	Vor	$Na_{16.18}K_{0.17}Ca_{4.54}(Mn,Fe)_{1.86}REE_{0.94}Zr_{2.70}Ti_{0.09}Nb_{0.20}Al_{0.10}Si_{25.84}O_{71.85}(OH)_{3.74}Cl_{0.35}$	Pfaff *et al.* (2008) and our unpublished data
Zirsinalite†	Zna	$Na_6CaZrSi_6O_{18}$	Pekov *et al.* (2009)
Aenigmatite	Aen	$Na_2Fe_5TiSi_6O_{20}$	Ideal composition
Astrophyllite	Ast	$Na_{1.21}K_{1.64}Ca_{0.19}(Fe,Mn)_{4.58}Zr_{0.12}Ti_{1.76}Nb_{0.13}Al_{0.18}Si_{7.88}(OH)_{4.38}F_{0.64}$	Piilonen *et al.* (2003)
Rinkite	Rin	$Na_{2.25}Ca_{3.38}Fe_{0.01}RE_{1.08}Zr_{0.05}T_{i0.61}Nb_{0.33}Si_4O_{28}F_{2.77}O_{1.23}$	Camara *et al.* (2011)
Nacareniobsite-(Ce)	Nrc	$Na_3Ca_3(Ce,La,Nd)Nb(Si_2O_7)_2OF_3$	Ideal composition
Neptunite	Npt	$Na_2KLi(Fe,Mn)_2Ti_2Si_8O_{24}$	Ideal composition
Lorenzenite	Lor	$Na_2Ti_2Si_2O_9$	Ideal composition
Murmanite‡	Mur	$Na_2Ti_2Si_2O_9{\cdot}2H_2O$	Ideal composition
Lovozerite§	Lov	$Na_3CaZrSi_6O_{16}(OH)_2$	Pekov *et al.* (2009)
Lomonosovite	Lom	$Na_5Ti_2(Si_2O_7)(PO_4)O_2$	Ideal composition
Steenstrupine-(Ce)	Ste	$Na_{14}Ce_6Mn_2Fe_2(Zr,Th)(Si_6O_{18})_2(PO_4)_7{\cdot}3H_2O$	Khomyakov & Sørensen (2001)
Vuonnemite	Vuo	$Na_{11}TiNb_2(Si_2O_7)_2(PO_4)_2O_3(F,OH)$	Ercit *et al.* (1998)
Epistolite	Epi	$Na_4Nb_2Ti_4(Si_2O_7)_2O_2(OH)_2(H_2O)_4$	Sokolova & Hawthorne (2004)
Apatite	Ap	$Ca_5(PO_4)_3F$	Ideal composition
Monazite	Mon	$(REE)PO_4$	Ideal composition
Vitusite-(Ce)	Vit	$Na_3REE(PO_4)_2$	Ideal composition
Natrophosphate	Nap	$Na_7(PO_4)_2F{\cdot}19H_2O$	Ideal composition

*Mineral of voronkovite-like composition whose structure has not been determined.
†Probably as precursor of lovozerite.
‡Probably replacement product after lomonosovite.
§Primary mineral and replacement product after zirsinalite.

arfvedsonite-bearing lujavrite (i.e. meso- to melanocratic agpaitic nepheline syenite) make up a sandwich horizon between roof and floor cumulates with offshoots into the roof cumulate and border group rocks (Ussing, 1912; Ferguson, 1964; Rose-Hansen & Sørensen, 2002; Sørensen, 2006; Sørensen *et al.*, 2011). Black, arfvedsonite-bearing lujavrite was emplaced after the kakortokite and naujaite cumulate sequences had formed. Extreme differentiation of lujavrite magma led locally to the formation of hyperagpaitic residual melts, which formed high-level intrusions of naujakasite and villiaumite lujavrite in the northernmost part of the complex, including the Kvanefjeld lujavrite with REE and U mineralization, and villiaumite and naujakasite lujavrite intrusions into the non-hyperagpaitic lujavrite of the sandwich horizon (Rose-Hansen & Sørensen, 2002; Sørensen *et al.*, 2011).

Hyperagpaitic rock types in the Ilímaussaq complex include villiaumite- and steenstrupine lujavrite (Rose-Hansen & Sørensen, 2002), naujakasite lujavrite (Sørensen *et al.*, 2011), pegmatites and veins (Danø & Sørensen, 1959; Bondam & Ferguson, 1962; Sørensen & Larsen, 2001; Markl & Baumgartner, 2002) and metasomatic alteration zones in the volcanic roof rocks (Sørensen & Larsen, 2001).

MINERALOGY OF THE AGPAITIC AND HYPERAGPAITIC ROCKS

A summary of magmatic mineral assemblages in agpaitic and hyperagpaitic rocks from Ilímaussaq compiled from our own observations and published sources is given in Table 2 (see table legend for references). Zircon, hiortdahlite and catapleiite are found only in the least alkaline intrusive rocks of the complex (Robles *et al.*, 2001; Marks & Markl, 2003), or as the products of post-magmatic alteration of eudialyte (Ussing, 1912; Karup-Møller *et al.*, 2010). Although interesting in their own right, these low-alkali assemblages are not important for the more advanced part of the magmatic evolution history considered here. Natrolite and other late or sub-solidus minerals are also not considered.

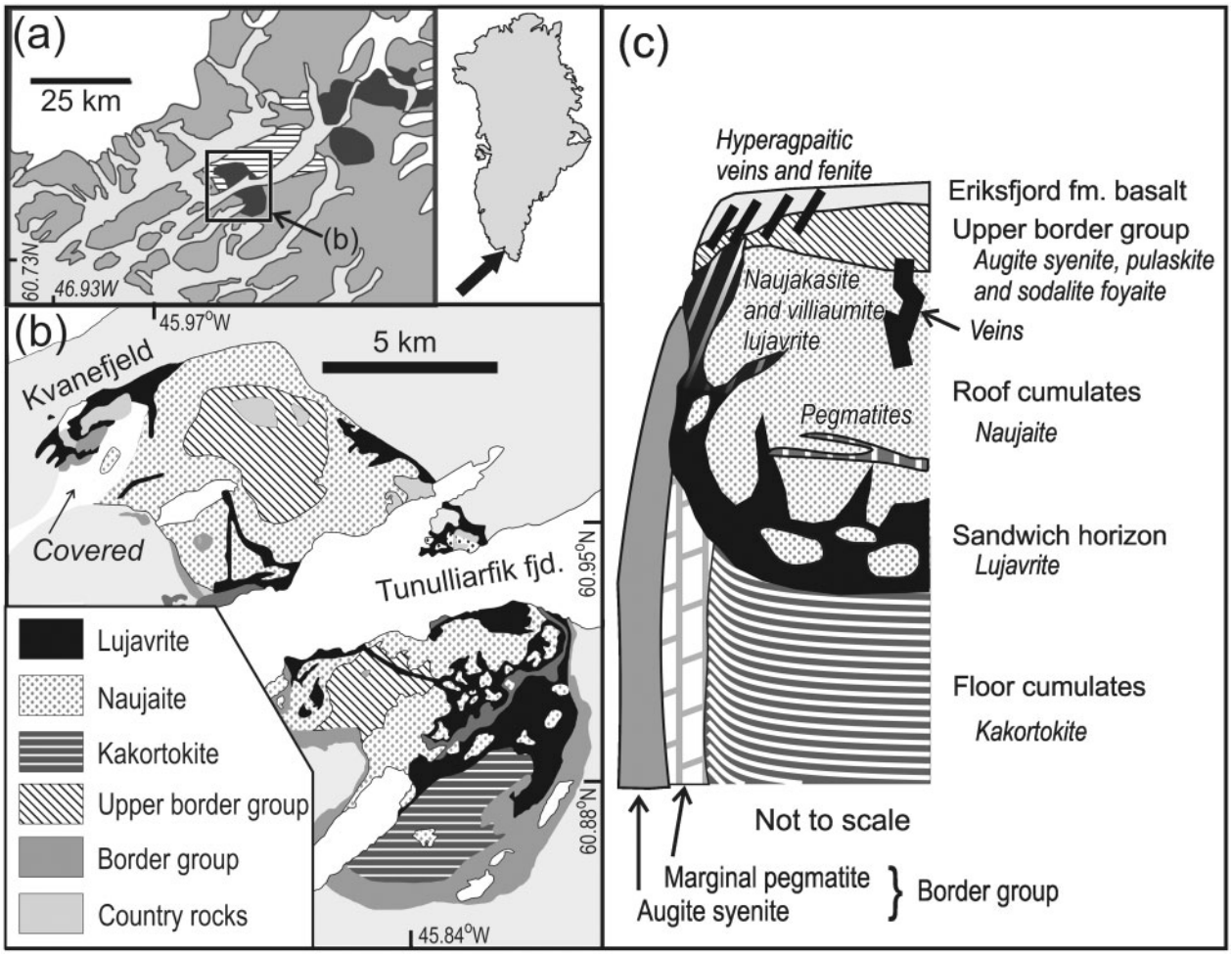

Fig. 1. Geological setting of the Ilímaussaq alkaline complex, South Greenland. (a) Geological sketch map of the eastern part of the Gardar Rift, showing Gardar intrusions (black) and supracrustal rocks (horizontal ruling). Pre-Gardar country rocks are shown with a grey fill; inland ice is white. (b) Simplified geological map of the Ilímaussaq alkaline complex, showing the main groups of intrusive rocks; adapted from Sørensen (2001). (c) Cross-section (not to scale) showing the principal features of the exposed part of the Ilímaussaq alkaline complex, based on Sørensen (2001) and Sørensen *et al.* (2011). The vertical extent is *c.* 1700 m.

Agpaitic rocks

The normal agpaitic rocks in the complex (sodalite foyaite, naujaite, kakortokite, and arfvedsonite and aegirine lujavrite) have primary magmatic mineral assemblages with major rock-forming minerals alkali feldspar (or albite + microcline), nepheline, arfvedsonite and/or aegirine, eudialyte, ±sodalite, ±fluorite, with sphalerite, apatite and polylithionite (among others) as important minor to accessory minerals. Sodalite is a primary magmatic mineral in the agpaitic rocks, and a major constituent of naujaite; primary sodalite is generally low in sulphur (Markl & Baumgartner, 2002). Analcime occurs as a late- to post-magmatic mineral in the agpaitic rock, commonly replacing magmatic feldspathoids. Eudialyte is the most important Zr-bearing mineral, reaching major proportions in the kakortokite. Aenigmatite is the most widespread titanium mineral in the agpaitic rocks, whereas neptunite is a minor mineral in naujaite and some varieties of lujavrite (Bailey *et al.*, 1993; Sørensen & Larsen, 2001). Rinkite occurs in sodalite foyaite, kakortokite and naujaite, where it is commonly associated with fluorite (or villiaumite; see below), whereas nacareniobsite-(Ce) is present in naujaite pegmatite and lujavrite (Ussing, 1912: Rønsbo *et al.*, 2014). Astrophyllite-group minerals occur in minor to accessory amounts in naujaite and lujavrite (Ussing, 1912; Sørensen, 1962) as well as in pegmatites and hydrothermal veins (Macdonald *et al.*, 2007; Hettmann *et al.*, 2014). However, most lujavrite does not carry separate Ti-rich minerals probably because of its relatively low concentration of TiO_2 (Bailey *et al.*, 2001). Phosphorus is low in the agpaitic rocks (≤0·06 wt % P_2O_5, Bailey *et al.*, 2001), and is hosted in accessory apatite. In naujaite, villiaumite forms part of late or secondary mineral assemblages with ussingite and analcime; that is, in assemblages with a clear hyperagpaitic affinity (Bondam & Ferguson, 1962).

Hyperagpaitic rocks

Hyperagpaitic lujavrites are somewhat variable in mineralogy, but are typically arfvedsonite lujavrites with microcline, albite, characteristic hyperagpaitic minerals

Table 2: Critical mineral assemblages in agpaitic and hyperagpaitic rocks in the Ilímaussaq alkaline complex

Rock type	Zrc	Hio	Cat	Eud	Ste	Vor	Lov* (Zna)	Aen	Ast	Rin	Lor	Mur† (Lom)	Vuo	Epi	Npt	Nrc	References
Plutonic rocks																	
Sodalite foyaite																	
Major minerals	Afs + Ne + Sod + Cpx + Amph + Fa ± Flu																1, 15
HFSE minerals				m				m	A	A							
Micro-kakortokite																	
Major minerals	Ab + Mc + Ne + Sod + Arf + Aeg																5, 13
HFSE minerals	m	m															
		m							m	m							
				m					m	m							
Kakortokite																	
Major minerals	Afs + Ne + Arf + Aeg ± Sod ± Flu																1, 15, 17
HFSE minerals			±S	M				m		m							
Naujaite																	1, 3, 15
Major minerals	Mc + Ab + Sod + Ne + Aeg + Arf ± Flu																
HFSE minerals				M				A	A	A				m	m	m	
Marginal pegmatite																	15, 17
Major minerals	Ab + Mc + Ne + Aeg/ Cpx + Arf/Amph + Flu ± Sod																
HFSE minerals	S	S	M					m									
Aegirine lujavrite																	1, 3, 15
Major minerals	Ab + Mc + Ne + Aeg ± Arf ± Sod ± Flu																
HFSE minerals																	
Arfvedsonite lujavrite																	
Major minerals	Ab + Mc + Ne + Arf ± Aeg ± Sod ± Flu																1, 3, 9, 15
HFSE minerals				M	**± m**			A	± A		± A		m	m	m	m	
Villiaumite lujavrite																	9, 11
Major minerals	Ab + Mc + Ne + Arf + **Vil** ± Sod ± Flu																
HFSE minerals				(m)	**M**								m				
Voronkovite lujavrite (low P_2O_5)																	19, 20
Major minerals	Ab + Mc + Ne + Arf+Aeg + **Vil**																
HFSE minerals						**M**											
Naujakasite lujavrite																	5, 14, 18, 20
Major minerals	Ab + Mc + **Nau** + Arf + **Vil** ± **Uss** ± **Nsl**‡																
HFSE minerals					**M**		**m**										
Pegmatites in naujaite																	2, 3, 17
Major minerals	Mc + Ab + Ne + Sod + Aeg + Arf																
HFSE minerals	± S		± S	M	**± m**			m		± m				m			
Veins																	
Late-magmatic veins																	4, 7, 12, 16
Major minerals	Mc, Av, Anl, Nat, **Uss**, **Vil**																
HFSE minerals				(m)	**m**				m					m			
Veins in roof rocks																	
Major minerals	Ne, Arf, Aeg																6, 7, 8, 10
HFSE minerals							**m**				A	**m**		m			

Mineral abbreviations are listed in Table 1. The plutonic rocks are listed in an approximate sequence of increasing agpaicitity. Bold type indicates hyperagpaitic indicator minerals. References: 1, Ussing (1912); 2, Danø & Sørensen (1959); 3, Sørensen (1962); 4, Bondam & Ferguson (1962); 5, Larsen & Steenfelt (1974); 6, Karup-Møller (1986*a*); 7, Karup-Møller (1986*b*); 8, Karup-Møller (1983); 9, Rønsbo *et al.* (1983); 10, Sørensen & Larsen (2001) and references therein; 11, Rose-Hansen & Sørensen (2002); 12, Markl & Baumgartner (2002); 13, Marks & Markl (2003); 14, Andersen & Sørensen (2005); 15, Sørensen (2006) and references therein; 16, Macdonald *et al.* (2007); 17, Karup-Møller *et al.* (2010), Karup-Møller & Rose-Hansen (2013); 18, Sørensen *et al.* (2011); 19, Pfaff *et al.* (2008); 20, present study.

*Lovozerite as replacment mineral after zirsinalite (Danø & Sørensen, 1959; Sørensen & Larsen, 2001), and as a primary mineral.

†Murmanite as replacement product after lononosovite (Karup-Møller, 1986*a*).

‡Natrosilite: inferred from solubility data (E. Sørensen, 1982; Sørensen & Larsen, 2001).

such as naujakasite and steenstrupine-(Ce), with minor aegirine and sphalerite (Fig. 2a–c), villiaumite (Fig. 3a), or villiaumite and steenstrupine-(Ce) (Fig. 2a). Eudialyte is in general not present in steenstrupine-(Ce)-bearing lujavrite. In phosphorus-poor hyperagpaitic lujavrite, however, steenstrupine-(Ce) is absent, and Zr is hosted in a sodium-rich eudialyte group mineral, probably voronkovite, based on microprobe analyses unsupported by structural data (Fig. 4). Voronkovite [Na_{15}(Na,Ca,REE)$_3$(Mn,Ca)$_3$$Fe_3Zr_3Si_{26}O_{72}(OH,O)_4$Cl·$H_2O$] is a Na-rich member of the eudialyte group with a lower symmetry than eudialyte *sensu stricto* (Khomyakov *et al.*, 2009), which is why we do not expect there to be a solid solution between the two minerals. Consequently, we treat them as two independent minerals despite their strong chemical similarities. In Ilímaussaq, this mineral coexists with albite, microcline, nepheline, arfvedsonite, aegirine and villiaumite.

The chlorine content of hyperagpaitic lujavrite is in general lower than in other lujavrite varieties (Bailey *et al.*, 2001); the abundance of sodalite is therefore variable. Hettmann *et al.* (2012) showed that sulphur substitutes for Cl in some sodalites, which may contribute to the lower Cl content of the hyperagpaitic lujavrites; elevated sulphur is also characteristic for sodalite formed in analcime ± ussingite-bearing hyperagpaitic hydrothermal veins (Markl & Baumgartner, 2002). Large, resorbed sodalite crystals in hyperagpaitic lujavrite, such as the one illustrated in Fig. 3b, may be xenocrysts derived from naujaite (Rose-Hansen & Sørensen, 2002). The presence of fluorite in some villiaumite lujavrites (Rose-Hansen & Sørensen, 2002) suggests a gradual transition rather than a sharp distinction between agpaitic and hyperagpaitic lujavrite in Ilímaussaq.

In naujakasite lujavrite, nepheline is scarce or absent; instead, magmatic naujakasite can amount to 80% of the rock (Andersen & Sørensen, 2005, and references therein). Natrosilite is present in naujakasite lujavrite that has not been exposed to air. Lovozerite group minerals (Fig. 3a) can be found as primary minerals in hyperagpaitic lujavrite, but have also been proposed as a replacement of zirsinalite, indicating that zirsinalite was also a stable mineral during magmatic crystallization (Danø & Sørensen, 1959; E. Sørensen, 1982; Sørensen & Larsen, 2001; Sørensen *et al.*, 2011). Ussingite occurs as a replacement product after alkali feldspar in some varieties of naujakasite lujavrite (Andersen & Sørensen, 2005).

The P_2O_5 content of the hyperagpaitic rocks is higher than in the agpaitic rocks (*c.* 0·5 wt %; Bailey *et al.*, 2001). Steenstrupine-(Ce) and other phosphosilicate and alkali phosphate minerals in these rocks, such as vitusite-(Ce), vuonnemite and natrophosphate (Fig. 2d), have crystallized early (Sørensen & Larsen, 2001, and references therein).

In the hyperagpaitic pegmatites and late-magmatic veins in the agpaitic rocks (Fig. 2c), ussingite is the most characteristic indicator mineral (Danø & Sørensen, 1959; Sørensen & Larsen, 2001; Markl & Baumgartner, 2002). Villiaumite- or villiaumite + ussingite-bearing veins were reported from naujaite and lujavrite by Bondam & Ferguson (1962). Ti-bearing minerals in ussingite-bearing veins include astrophyllite-group minerals, phosphosilicate minerals of the lomonosovite group, now replaced by murmanite, and epistolite (Karup-Møller, 1986*a*, 1986*b*; Sørensen & Larsen, 2001; Macdonald *et al.*, 2007). Rinkite is not present in hyperagpaitic rocks in Ilímaussaq, but it has been reported from hyperagpaitic pegmatite in Khibina (Yakovenchuk *et al.*, 2005), and 'mosandrite' with composition $Na_2Ca_4CeTiSi_4O_{15}F_3$ is a widespread mineral in hyperagpaitic rocks in both Lovozero and Khibina (Khomyakov, 1995); this composition is close to that of rinkite reported from agpaitic rocks in Ilímaussaq (Table 1). The distinction between rinkite and mosandrite has been very problematic (Sokolova & Camara, 2008; Bellezza *et al.*, 2009*a*, 2009*b*). However, Bellezza *et al.* (2009*a*) could demonstrate that the type mosandrite from the Langesundsfjord pegmatites in the Oslo Rift, Norway is a cation-deficient and hydrated member of the rinkite group. Accepting this definition, the anhydrous mineral from Khibina and Lovozero is rinkite rather than mosandrite. Rinkite should therefore be considered a potential mineral in both agpaitic and hyperagpaitic lujavrite.

Critical mineral assemblages for the agpaitic–hyperagapaitic transition

Normal agpaitic rocks (kakortokite, naujaite, ordinary lujavrite) are characterized by mineral assemblages with albite, microcline, arfvedsonite and/or aegirine, with eudialyte as the main zirconium-bearing mineral, whereas aenigmatite, astrophyllite and rinkite must be considered potential host minerals for titanium. With increasing agpaiticity, villiaumite appears as a characteristic mineral, naujakasite and ussingite form instead of nepheline and albite, respectively, and eventually natrosilite crystallizes. In this process, zirconium will be incorporated in steenstrupine-(Ce) or voronkovite instead of eudialyte, and titanium in vuonnemite. The critical mineral assemblages that mark this transition are given in Table 2.

CHEMOGRAPHIC MODELLING OF THE AGPAITIC–HYPERAGPAITIC TRANSITION

Agpaitic and hyperagpaitic igneous rocks are complex systems, in which elements that are trace components in most igneous rocks are enriched to minor to major element concentration level. A full chemographic analysis of the system would therefore require more than 20 components, which are too many to handle. Andersen & Sørensen (2005) could model a simplified naujakasite lujavrite in terms of only six components (Na–Al–Fe–Si–O–H). Whereas this was sufficient to understand the stability relationships of naujakasite, it omitted components such as zirconium, titanium,

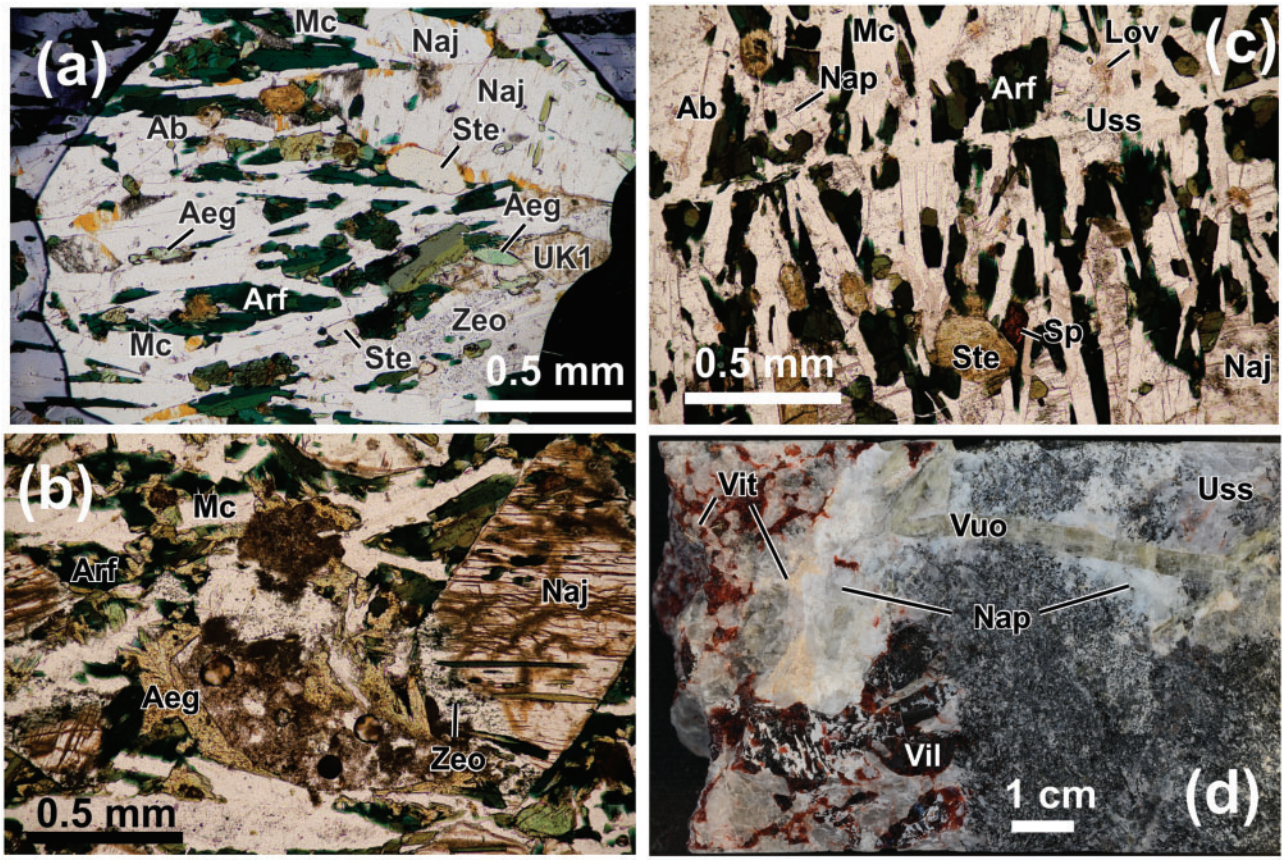

Fig. 2. (a-c) Photomicrographs of hyperagpaitic rocks from Kvanefjeld, Ilímaussaq alkaline complex. (a) Naujakasite lujavrite (drill core K_M002_106) with albite (Ab) and microcline (Mc), arfvedsonite (Arf), naujakasite (Naj) and minor steenstrupine-(Ce) (Ste) and aegirine (Aeg). Zeo is a zeolite mineral, and UK1 an unknown mineral species. (b) Naujakasite lujavrite (drill core K_M010_102) with a large crystal of naujakasite (Naj), microcline (Mc) and arfvedsonite (Arf) with aegirine (Aeg) partly replacing arfvedsonite and an unidentified zeolite mineral (Zeo) replacing naujakasite. (c) Naujakasite lujavrite (drill core K_M012_150) crosscut by a vein of ussingite (Uss). The lujavrite contains natrophosphate (Nap), lovozerite (Lov), steenstrupine-(Ce) (Ste) and sphalerite (Sp) that crystallized before the ussingite vein formed. (d) Photograph of a split drill core (K_144_163.2) showing a hyperagpaitic lujavrite with vuonnemite (Vuo) in a vein with ussingite (Uss), villiaumite (Vil), natrophosphate (Nap) and vitusite-(Ce) (Vit).

chlorine and fluorine, which are essential for the evolution of the lujavrite magma.

By combining the REE with Y, Hf with Zr, Ta with Nb, and Mn with Fe^{2+}, it is possible to describe the most important phase reactions in the agpaitic and hyperagpaitic melts in terms of the 12 simplified oxide components $NaO_{0.5}$, $KO_{0.5}$, CaO, FeO, $FeO_{1.5}$, $REEO_{1.5}$, ZrO_2, TiO_2, $NbO_{2.5}$, $AlO_{1.5}$, SiO_2 and $HO_{0.5}$, and two volatile exchange components $FO_{-0.5}$ and $ClO_{-0.5}$. In addition, $PO_{2.5}$ must be included to account for reactions including phosphosilicate minerals such as steenstrupine-(Ce) and vuonnemite. By this choice of components some elements that are important in minerals in hyperagpaitic rocks are left out of consideration (e.g. U, Th, Be, Li, C).

The REE are minor components in eudialyte and rinkite, and essential in a range of minor to accessory minerals, such as steenstrupine-(Ce), vitusite-(Ce) and nacareniobsite-(Ce); the activities of these components can be considered to be controlled by external buffering without detrimental effects. The same applies to niobium, which is, however, essential in vuonnemite and nacareniobsite-(Ce). Calcium is a problematic component in these rocks, in the sense that none of the ordinary rock-forming minerals crystallizing at the transition from agpaitic to hyperagpaitic conditions (nepheline, albite, naujakasite, arfvedsonite, microcline) have essential Ca, whereas minerals such as eudialyte and rinkite have. The clinopyroxene in hyperagpaitic rocks is aegirine without significant Ca (Larsen, 1976; Andersen & Sørensen, 2005). As a consequence, CaO is left unconstrained in the model calculations. Reactions involving arfvedsonite, naujakasite and eudialyte are dependent on oxygen fugacity. Oxygen fugacity is not considered explicitly in the model. For most of the evolution of the agpaitic magma in Ilímaussaq, f_{O2} is low, well below the un-displaced quartz–fayalite–magnetite (QFM) buffer (Larsen, 1976), but increases towards the end of the crystallization history (Markl *et al.*, 2001). The presence of naujakasite and arfvedsonite is consistent with a generally low oxygen fugacity level in naujakasite lujavrite (Andersen & Sørensen, 2005).

A petrogenetic grid for the agpaitic to hyperagpaitic transition in Ilímaussaq

A multidimensional petrogenetic grid for the agpaitic and hyperagpaitic rocks can be constructed from the

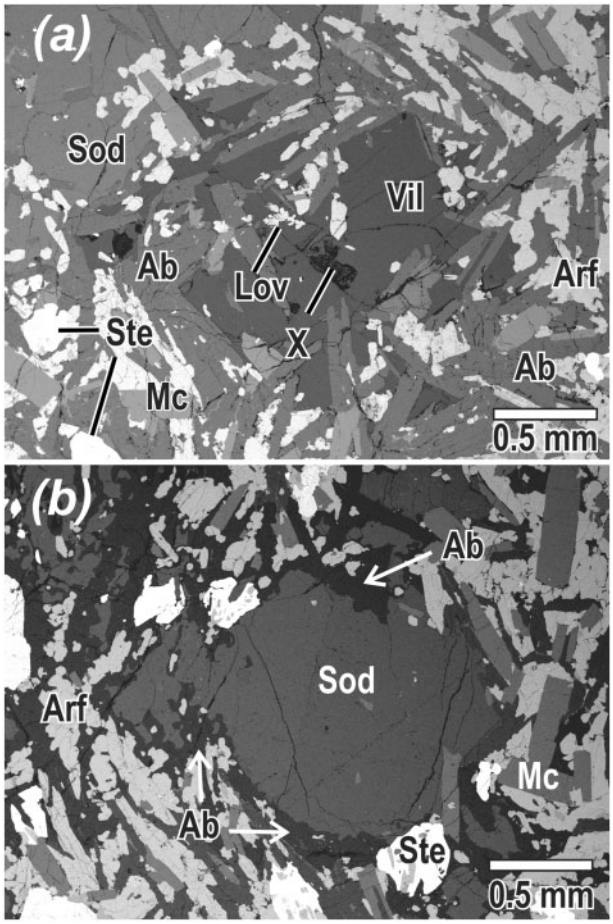

Fig. 3. Backscattered electron images of villiaumite–steenstrupine lujavrite from the Kvanefjeld mine dump, Ilímaussaq alkaline complex. (a) Interstitial villiaumite (Vil) between crystals of albite (Ab, dark), microcline (Mc, medium grey), arfvedsonite (Arf, light grey) and steenstrupine-(Ce) (Ste, white). A large aggregate of sodalite crystals occurs in the upper left corner (Sod). × marks a pit after a partially dissolved crystal of a Na–P-bearing mineral, most probably dorfmanite [$Na_2(PO_3OH)_2{\cdot}2H_2O$]. The crystal aggregate Lov consists of partly altered lovozerite. (b) A large, corroded crystal of sodalite (Sod) surrounded by a rim of albite (Ab) set in a matrix of microcline (Mc), arfvedsonite (Arf), albite and steenstrupine-(Ce) (Ste).

observed mineral assemblages by applying the principles of Schreinemakers analysis as outlined by Zen (1966) and White *et al.* (2008). The approach has been applied to the agpaitic (but not to the hyperagpaitic) rocks of Ilímaussaq by Marks *et al.* (2011). Andersen *et al.* (2010) constructed a three-dimensional (3D) petrogenetic grid in log a_{Nds}–log a_{H2O}–log a_{HF} space for mildly agpaitic nepheline syenite pegmatites in the Oslo Rift, Norway, addressing the transition from miaskitic to agpaitic conditions. In the present study, we have applied the same method to construct 2D and 3D petrogenetic grids relating to the agpaitic–hyperagpaitic transition. Excess sodium [expressed as the $Na_2Si_2O_5$ sodium disilicate component (Nds) of the melt] is one of the main parameters to control this transition (Andersen & Sørensen, 2005, and references therein).

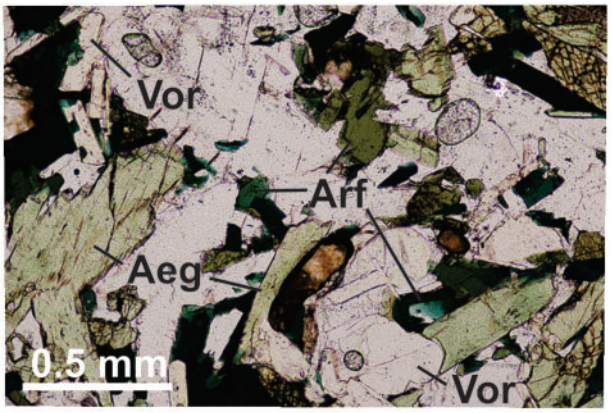

Fig. 4. Naujakasite-free, hyperagpaitic lujavrite with aegirine (Aeg), arfvedsonite (Arf) and voronkovite (Vor). Drill core K_M012_200.

In addition, halogen activities (expressed as a_{HCl} and a_{HF}), a_{H2O} and a_{P2O5} are parameters that need to be considered.

Low-variance phase equilibrium reactions that are needed to construct the grid have been balanced by matrix inversion using the built-in algorithm of Microsoft Excel (Table 3), and the corresponding divariant planes and univariant lines in isothermal–isobaric 3D log a_{Nds}–log a_{H2O}–log a_{HF}, log a_{Nds}–log a_{H2O}–log a_{HCl} or log a_{Nds}–log a_{H2O}–log a_{P2O5} space in agreement with observed mineral assemblages have been constructed using the method described by Andersen *et al.* (2010). The transition from agpaitic to hyperagpaitic conditions influences the major, non-HFSE-bearing mineral assemblages of the rocks, as well as the zirconium-, titanium- and phosphorus-bearing minerals.

The major, non-HFSE silicate minerals

As a first step, a grid for the HFSE-free sub-system $NaO_{0.5}$–FeO–$FeO_{1.5}$–$AlO_{1.5}$–SiO_2–$HO_{0.5}$–$FO_{-0.5}$–$ClO_{-0.5}$ is established. The magmatic mineral assemblages that need to be considered are as follows: (1) the normal mineral assemblage of a nepheline syenite: nepheline + microcline + albite + arfvedsonite ± sodalite; (2) the simplified assemblage of a naujakasite lujavrite: naujakasite + albite + microcline + arfvedsonite ± sodalite; (3) ussingite-bearing assemblages; (4) saturation surfaces for sodalite, fluorite, villiaumite and natrosilite.

The stability relationships of the major silicate minerals are defined by reactions (a1)–(a7) in Table 3, all of which are independent of fluorine and chlorine, and are illustrated in a section at constant a_{HF} in Fig. 5a. The ordinary nepheline syenite assemblage with albite + nepheline is unstable at elevated a_{Nds}. At elevated a_{H2O}, albite and nepheline are replaced by analcime [reaction (a6) in Table 3]. Ussingite is related to albite and nepheline by reaction (a1), and to analcime by reaction (a7), which truncates the analcime field at elevated a_{Nds}. Because ussingite in Ilímaussaq has formed at the expense of albite rather than nepheline, Uss + Ne + Mc +

Table 3: Divariant reactions defining the petrogenetic grid

(a) *System $NaO_{0.5}$–$KO_{0.5}$–FeO–$FeO_{1.5}$–$AlO_{1.5}$–SiO_2–$HO_{0.5}$*
(a1) Albite–ussingite
0·63 Ab + 0·13 Ne + 0·50 H_2O + 0·50 $Na_2Si_2O_5$ = 1·00 Uss + 0·13 Mc

(a2) Nepheline–naujakasite
1·38 Ab + 0·88 Ne + 0·20 Arf + 0·70 $Na_2Si_2O_5$ = 1·00 Naj + 0·88 Mc + 0·2 H_2O + 0·05 O_2

(a3) Naujakaiste–ussingite–albite
2·33 Uss + 0·07 Arf = 1·00 Ab + 0·33 Naj + 1·23 H_2O + 0·93 $Na_2Si_2O_5$ + 0·02 O_2

(a4) Naujakasite–ussingite–nepheline
1·67 Naj + 1·00 Mc + 2·17 H_2O + 0·67 $Na_2Si_2O_5$ + 0·08 O_2 = 1·00 Ne + 3·67 Uss + 0·33 Arf

(a5) Natrosilite saturation
$Na_2Si_2O_5$ = Nsl

(a6) Albite–nepheline–analcime
1·60 Anl + 0·20 Mc = 1·00 Ab + 0·2 Ne + 1·6 H_2O

(a7) Analcime–ussingite
1·00 Anl + 0·50 $Na_2Si_2O_5$ = 1·00 Uss + 0·5 H_2O

(b) *System $NaO_{0.5}$–$KO_{0.5}$–FeO–$FeO_{1.5}$–$AlO_{1.5}$–SiO_2–$HO_{0.5}$–$ClO_{-0.5}$*
(b1) Albite–nepheline–sodalite
0·38 Ab + 0·88 Ne + 0·50 $Na_2Si_2O_5$ + 1·00 HCl = 1·00 Sod + 0·88 Mc + 0·5 H_2O

(b2) Naujakasite–sodalite–albite
1·00 Naj + 1·00 HCl + 0·05 O_2 = 1·00 Sod + 1 Ab + 0·2 Arf + 0·3 H_2O + 0·2 $Na_2Si_2O_5$

(b3) Ussingite–nepheline–sodalite
0·80 Ne + 0·60 Uss + 0·20 $Na_2Si_2O_5$ + 1·00 HCl = 1·00 Sod + 0·8 Mc + 0·8 H_2O

(b4) Ussingite–sodalite–albite
0·14 Sod + 0·57 Ab + 0·57 H_2O + 0·43 $Na_2Si_2O_5$ = 1·00 Uss + 0·14 HCl

(b5) Analcime–nepheline–sodalite
0·80 Ne + 0·60 Anl + 0·50 $Na_2Si_2O_5$ + 1·00 HCl = 1·00 Sod + 0·8 Mc + 1·1 H_2O

(c) *Fluoride mineral saturation*
(c1) Fluorite
1·00 CaO + 2·00 HF = 1·00 Flu + 1 H_2O

(c2) Villiaumite–nepheline–albite
0·13 Ne + 0·50 $Na_2Si_2O_5$ + 1·00 HF = 1·00 Vil + 0·38 Ab + 0·13 Mc + 0·5 H_2O

(c3) Villiaumite–ussingite
0·20 Ne + 0·80 $Na_2Si_2O_5$ + 1·00 HF = 1·00 Vil + 0·6 Uss + 0·2 Mc + 0·2 H_2O

(c4) Villiaumite–naujakasite
0·14 Naj + 0·40 $Na_2Si_2O_5$ + 1·00 HF + 0·01 O_2 = 1·00 Vil + 0·57 Ab + 0·03 Arf + 0·47 H_2O

(d) *Stability field of eudialyte*
(d1) Eudialyte–zircon
0·37 Eud + 0·24 Ne + 0·10 H_2O + 0·06 O_2 = 1·00 Zrc + 0·71 Ab + 0·3 Mc + 1·99 CaO + 0·23 Arf + 0·04 Nb_2O_5 + 0·1 REE_2O_3 + 2·37 $Na_2Si_2O_5$ + 0·49 HCl

(d2) Eudialyte–catapleiite
0·37 Eud + 0·16 Ne + 2·10 H_2O + 0·06 O_2 = 1·00 Cat + 0·49 Ab + 0·23 Mc + 1·69 CaO + 0·23 Arf + 0·04 Nb_2O_5 + 0·09 REE_2O_3 + 1·67 $Na_2Si_2O_5$ + 0·49 HCl

(d3) Eudialyte–hiortdahlite
0·37 Eud + 0·14 Ne + 0·04 Npt + 0·03 Nb_2O_5 + 4·71 HF + 0·04 O_2 = 1·00 Hio + 0·36 Ab + 0·22 Mc + 0·96 CaO + 0·17 Arf + 0·09 REE_2O_3 + 2·3 H_2O + 1·62 $Na_2Si_2O_5$ + 0·49 HCl + 0·02 Plt

(d4a) Eudialyte–steenstrupine-(Ce)–albite–nepheline
0·37 Eud + 1·11 Ne + 0·57 Arf + 2·90 REE_2O_3 + 2·30 H_2O + 3·43 $Na_2Si_2O_5$ + 0·36 O_2 + 4·00 P_2O_5 = 1·00 Ste + 3·34 Ab + 1·18 Mc + 1·99 CaO + 0·04 Nb_2O_5 + 0·49 HCl

(d4b) Eudialyte–steenstrupine-(Ce)–naujakasite–nepheline
0·37 Eud + 1·27 Naj + 0·32 Arf + 2·90 REE_2O_3 + 2·56 H_2O + 2·54 $Na_2Si_2O_5$ + 0·42 O_2 + 4·00 P_2O_5 = 1·00 Ste + 5·09 Ab + 0·06 Mc + 1·99 CaO + 0·04 Nb_2O_5 + 0·49 HCl

(e) *Voronkovite and zirsinalite stability fields*
(e1) Voronkovite–eudialyte
1·00 Vor + 0·22 Ab + 0·06 Mc + 0·85 CaO + 0·98 HCl + 0·30 Arf = 1·00 Eud + 0·06 Ne + 0·3 Aeg + 0·07 TiO_2 + 0·21 REE_2O_3 + 1·67 H_2O + 1·10 $Na_2Si_2O_5$

(e2) Voronkovite–steenstrupine-(Ce)
0·37 Vor + 1·09 Ne + 1·67 Aeg + 2·83 REE_2O_3 + 2·04 H_2O + 2·66 $Na_2Si_2O_5$ + 0·33 Arf + 4·00 P_2O_5 = 1·00 Ste + 3·26 Ab + 1·16 Mc 1·68 CaO + 0·03 TiO_2 + 0·04 Nb_2O5 + 0·13 HCl

(continued)

Table 3: Continued

(e3) Voronkovite–zirsinalite
2·70 Zna + 2·72 Ab + 1·10 Mc + 1·84 CaO + 0·09 TiO_2 + 0·10 Nb_2O_5 + 0·47 REE_2O_3 + 1·23 H_2O + 0·35 HCl + 0·47 Arf = 1·00 Vor + 0·93 Ne + 0·47 Aeg + 0·44 $Na_2Si_2O_5$

(e4a) Zirsinalite–steenstrupine-(Ce)–nepheline
1·00 Zna + 0·75 Ne + 1·50 Aeg + 3·00 REE_2O_3 + 2·50 H_2O + 2·50 $Na_2Si_2O_5$ + 0·50 Arf + 4·00 P_2O_5 = 1·00 Ste + 2·25 Ab + 0·75 Mc + 1 CaO

(e4b) Zirsinalite–steenstrupine-(Ce)–naujakasite
1·00 Zna + 0·86 Naj + 1·71 Aeg + 3·00 REE_2O_3 + 2·71 H_2O + 1·86 $Na_2Si_2O_5$ + 0·29 Arf + 4·00 P_2O_5 = 1·00 Ste + 3·43 Ab + 1 CaO

(e5a) Zirsinalite–eudialyte–nepheline
2·70 Zna + 2·94 Ab + 1·16 Mc + 2·69 CaO + 0·02 TiO_2 + 0·10 Nb_2O_5 + 0·26 REE_2O_3 + 1·33 HCl + 0·77 Arf = 1·00 Eud + 0·99 Ne + 0·77 Aeg + 0·44 H_2O + 1·54 $Na_2Si_2O_5$

(e5b) Zirsinalite–eudialyte–naujakasite
2·70 Zna + 4·50 Ab + 0·17 Mc + 2·69 CaO + 0·02 TiO_2 + 0·10 Nb_2O_5 + 0·26 REE_2O_3 + 1·33 HCl + 1·05 Arf = 1·00 Eud + 1·13 Naj + 1·05 Aeg + 0·72 H_2O + 0·70$Na_2Si_2O_5$

(f) *Titanium minerals*
(f1) Aenigmatite-in
0·13 Ne + 1·00 TiO_2 + 1·00 Arf = 1·00 Aen + 0·38 Ab + 0·13 Mc + 0·25 O_2 + 1 H_2O + 0·50 $Na_2Si_2O_5$

(f2) Astrophyllite-in
0·04 Eud + 0·31 Ne + 1·28 Mc + 1·50 TiO_2 + 0·05 Nb_2O_5 + 0·35 H_2O + 0·60 HF + 1·34 Arf = 1·00 Ast + 2·33 Ab + 0·18 CaO + 0·33 O_2 + 0·01 REE_2O_3 + 0·98 $Na_2Si_2O_5$ + 0·05 HCl

(f3) Vuonnemite-in
(f3a) Vuonnemite–albite
0·88 Ne + 1·00 TiO_2 + 1·00 Nb_2O_5 + 5·50 $Na_2Si_2O_5$ + 1·00 HF + 1·00 P_2O_5 = 1·00 Vuo + 2·63 Ab + 0·88 Mc + 0·5 H_2O

(f3b) Vuonnemite–ussingite
1·40 Ne + 1·00 TiO_2 + 1·00 Nb_2O_5 + 1·60 H_2O + 7·60 $Na_2Si_2O_5$ + 1·00 HF + 1·00 P_2O_5 = 1·00 Vuo + 4·2 Uss + 1·4 Mc

(f4) Epistolite-in
0·08 Uss + 0·03 Mc + 0·27 CaO + 0·01 O_2 + 1·04 TiO_2 + 0·96 Nb_2O_5 + 1·67 H_2O + 1·83 $Na_2Si_2O_5$ + 0·02 Arf = 1·00 Epi + 0·03 Ne

(f5) Rinkite-in
0·02 Eud + 0·61 Ab + 0·20 Mc + 3·29 CaO + 0·61 TiO_2 + 0·16 Nb_2O_5 + 0·53 REE_2O_3 + 1·01 $Na_2Si_2O_5$ + 2·77 HF = 1·00 Rin + 0·2 Ne + 1·38 H_2O + 0·02 HCl + 0·01 Arf

(f6) Rinkite–astrophyllite
0·81 Ne + 0·79 Mc + 2·46 Rin + 3·75 H_2O + 0·01 HCl + 1·36 Arf = 1·00 Ast + 0·01 Eud + 3·82 Ab + 8·26 CaO + 0·34 O_2 + 0·36 Nb_2O_5 + 1·32 REE_2O_3 + 3·45 Na2Si2O5 + 6·21 HF

(f7) Rinkite–aenigmatite
0·46 Ne + 1·64 Rin + 1·27 H_2O + 0·04 HCl + 1·01 Arf = 1·00 Aen + 0·03 Eud + 1·37 Ab + 0·45 Mc + 5·39 CaO + 0·25 O_2 + 0·27 Nb_2O_5 + 0·88 REE_2O_3 + 2·15 $Na_2Si_2O_5$ + 4·54 HF

(f8) Rinkite–vuonnemite
(f8a) Rinkite–vuonnemite–eudialyte–albite
1·21 Ne + 1·64 Rin + 0·73 Nb_2O_5 + 1·77 H2O + 3·85 $Na_2Si_2O_5$ + 0·04 HCl + 0·01 Arf + 1·00 P_2O_5 = 1·00 Vuo + 0·03 Eud + 3·62 Ab + 1·2 Mc + 5·39 CaO + 0·88 REE_2O_3 + 3·54 HF

(f8b) Rinkite–vuonnemite–steenstrupine-(Ce)–albite
1·29 Ne + 0·02 O_2 + 1·64 Rin + 0·73 Nb_2O_5 + 1·94 H_2O + 4·11 $Na_2Si_2O_5$ + 0·06 Arf + 1·31 P_2O_5 = 1·00 Vuo + 0·08 Ste + 3·87 Ab + 1·29 Mc + 5·54 CaO + 0·65 REE_2O_3 + 3·54 HF

(f8c) Rinkite–vuonnemite–steenstrupine-(Ce)–ussingite
2·07 Ne + 0·02 O_2 + 1·64 Rin + 0·73 Nb_2O_5 + 5·04 H_2O + 7·21 $Na_2Si_2O_5$ + 0·06 Arf + 1·31 P_2O_5 = 1·00 Vuo + 0·08 Ste + 6·2 Uss + 2·07 Mc + 5·54 CaO + 0·65 REE_2O_3 + 3·54 HF

(g) *Phosphate mineral reactions*
(g1) Natrophosphate-in
(g1a) 4·50 Uss + 1·50 HCl + 1·00 Nap = 1·00 P_2O_5 + 1·5 Sod + 22 H_2O + 4·5 $Na_2Si_2O_5$ + 1 Vil

(g1b) 7·50 Uss + 5·00 CaO + 2·50 HCl + 1·50 Nap = 1·00 Ap + 2·5 Sod + 33·5 H_2O + 7·5 $Na_2Si_2O_5$ + 0·5 Vil

(g2) Vitusite-(Ce)-in

(g2a) 2·25 Uss + 0·75 HCl + 1·00 Vit = 1·00 P_2O_5 + 0·75 Sod + 0·5 REE_2O_3 + 1·5 H_2O + 2·25 $Na_2Si_2O_5$

(g2b) 7·50 Uss + 5·00 CaO + 1·00 Vil + 2·50 HCl + 3·00 Vit = 1·00 Ap + 2·5 Sod + 3 Mon + 5 H_2O + 7·5 $Na_2Si_2O_5$

(g3) Vitusite-(Ce)–natrophosphate
(g3a) 0·75 Sod + 20·50 H_2O + 2·25 $Na_2Si_2O_5$ + 1·00 Vil + 1·00 Vit = 1·00 NaP + 2·25 Uss + 0·5 REE_2O_3 + 0·75 HCl

(g3b) 1·00 Mon + 0·50 Nap = 1·00 Vit + 9·5 H_2O + 0·5 Vil

Mineral abbreviations and formulae are given in Table 1.

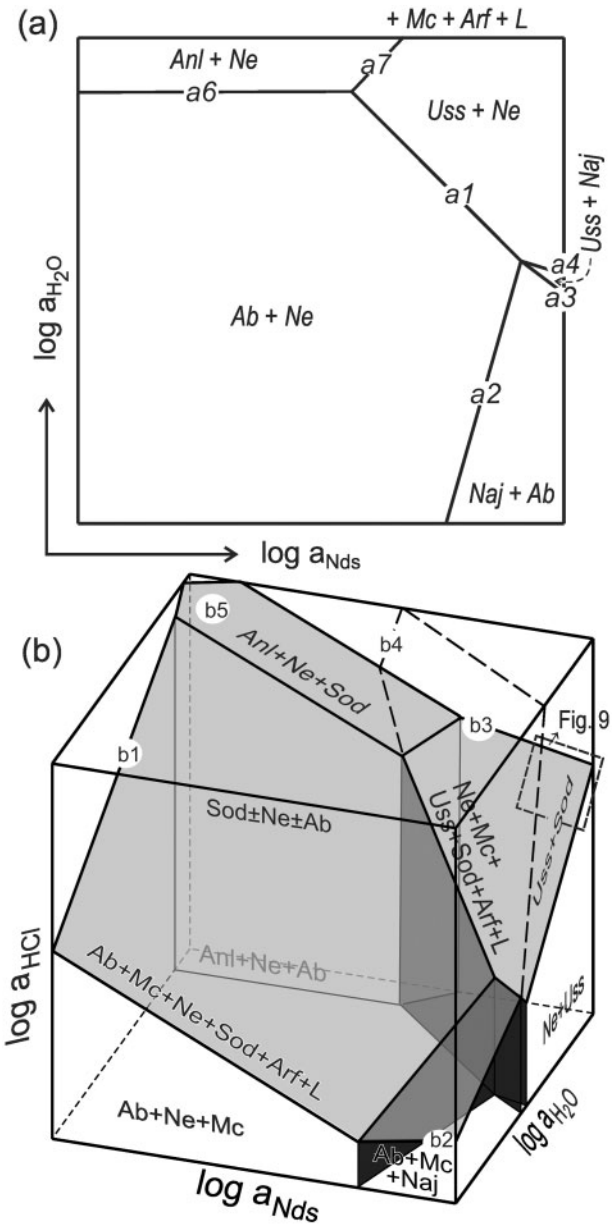

Fig. 5. (a) log a_{Nds}–log a_{H2O} (where Nds is the $Na_2Si_2O_5$ component of the magma) section at constant pressure, temperature, a_{HCl} and a_{HF}, showing the relative stability fields of major silicate mineral assemblages in an HFSE-free agpaitic to hyperagpaitic system at conditions where neither sodalite nor fluoride minerals are stable. The presence of peralkaline melt (L), microcline (Mc) and arfvedsonite (Arf) is assumed. Lines are labeled with reaction numbers from Table 3. (b) A 3D rendering of an isobaric–isothermal petrogenetic grid in log a_{Nds}–log a_{H2O}–log a_{HCl} space, showing the sodalite-saturation surface and volumes in which sodalite + ussingite would be stable in systems without albite or nepheline. Planes are labeled with reaction numbers from Table 3.

Arf ± Sod and Ab + Ne + Mc + Arf ± Sod are assumed to be stable assemblages, rather than the albite + ussingite-bearing alternative Ab + Uss + Mc + Arf ± Sod, which has not been observed. Ussingite is stable at elevated a_{H2O} and a_{Nds}, and naujakasite at elevated a_{Nds} and lower water activity (Fig. 5a). Ussingite and naujakasite coexist in a narrow range of water activity at high a_{Nds} limited at low and high water activity by reactions (a3) and (a4), respectively. The maximum a_{Nds} attainable in this system is defined by the presence of stable natrosilite [reaction (a5)], along a plane parallel to the log a_{H2O}–log a_{HCl} side of the diagram in Fig. 5b. Sodalite is stable at elevated a_{HCl}; the assemblages Sod + Ne + Mc + Ab + Arf + L, Sod + Ne + Mc + Anl + Arf + L, Sod + Naj + Ab + Mc + Arf + L and Sod + Ne + Uss + Arf + L form intersecting planes [reactions (b1), (b2), (b3) and (b5) in Table 3] defining a sloping surface over the sodalite-free system (Fig. 5b). This surface represents the maximum a_{HCl} attainable in a system where sodalite coexists with alkali feldspar, analcime, ussingite and nepheline. Ussingite without nepheline is stable to higher a_{HCl}, limited by reaction (b4).

Fluorite, villiaumite and maximum HF activity

The maximum HF activity in the system is reached where the silicate minerals react with melt or magmatic fluid to form fluorite or villiaumite. The fluoride-saturated, nominally divariant assemblages (Ne + Ab + Mc + Arf + Flu + L, Ne + Ab + Mc + Arf + Vil + L, Naj + Ab + Mc + Arf + Vil + L, Ne + Uss + Mc + Arf + Vil + L and Naj + Uss + Ab + Mc + Arf + Vil + L) form an inclined 'roof' over the grid in log a_{Nds}–log a_{H2O}–log a_{HF} space defined by reactions (c1), (c2), (c3) and (c4) in Table 3 that cannot be penetrated by closed-system differentiation processes, as fluoride minerals would form in response (Fig. 6). Because fluorite stability [reaction (c1)] is dependent on calcium activity, the fluorite saturation plane will shift towards higher a_{HF} with reduced a_{CaO} (Fig. 6). The villiaumite-bearing assemblages define divariant planes with different spatial orientation, joined along the univariant lines defined by assemblages in the fluorine-free system (Figs 5a and 6). The dependence of fluorite stability on a_{CaO} has the implication that there is no sharply defined minimum limit for the a_{Nds} required to stabilize villiaumite in the system: at low a_{CaO}, the fluorite–villiaumite univariant will be displaced to a_{Nds} values lower than would be expected in a system where a_{CaO} is controlled by internal buffering, but at the same time to higher a_{HF}.

Zirconium minerals

The stability volumes of eudialyte and other zirconium-bearing minerals are constructed within the grid defined by the major, HFSE-free minerals. Because eudialyte has essential chlorine, eudialyte has its maximum stability at the highest attainable a_{HCl} (i.e. in a system that is saturated in sodalite); the grid for zirconium-bearing minerals in Fig. 6 has been drawn assuming sodalite saturation. Under such conditions, eudialyte is stable over most of the volume considered here (Fig. 6). Towards low a_{Nds}, it is replaced by zircon [reaction (d1)], except at high a_{H2O}, where catapleiite is the stable phase [reaction (d2)]. The zircon- and catapleiite-forming reactions are independent of a_{HF}. In mildly agpaitic systems, hiortdahlite is stable at low a_{Nds} and

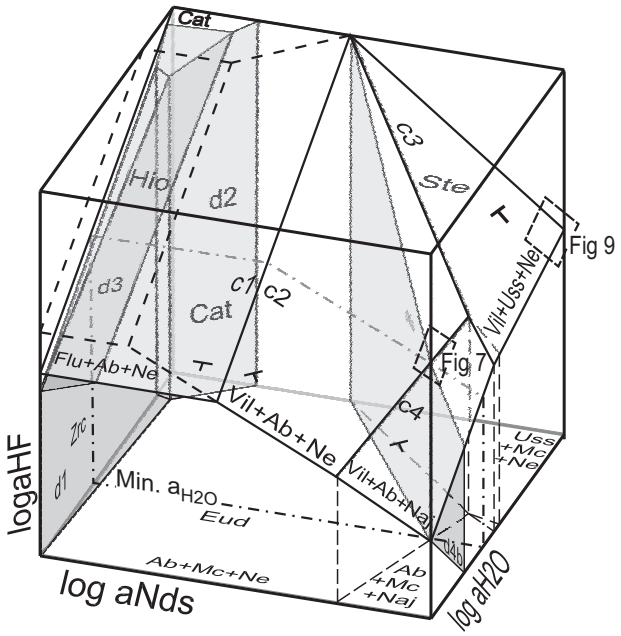

Fig. 6. A 3D rendering of an isobaric–isothermal petrogenetic grid for eudialyte and other Zr-rich minerals in Ilímaussaq lujavrite and hyperagpaitic rocks in log a_{Nds}–log a_{H2O}–log a_{HF} space. Albite or ussingite, nepheline or naujakasite, arfvedsonite, sodalite and a silicate liquid are assumed to be present. The villiaumite saturation plane is defined by three segments with different spatial orientation, as indicated by strike-and-dip symbols. The stability of villiaumite is tied to major, rock-forming minerals in the HFSE-free system, so that they are truly divariant surfaces. Because the CaO activity at the agpaitic to hyperagpaitic transition stage in Ilímaussaq is unconstrained by phase reactions involving major, rock-forming minerals, the fluorite-in reaction is not truly divariant, and the position of the fluorite saturation surface is shown at two arbitrary levels of CaO activity. The dashed-line rectangles show the positions of detailed diagrams shown in Figs 7 and 9. Planes are labeled with reaction numbers from Table 3.

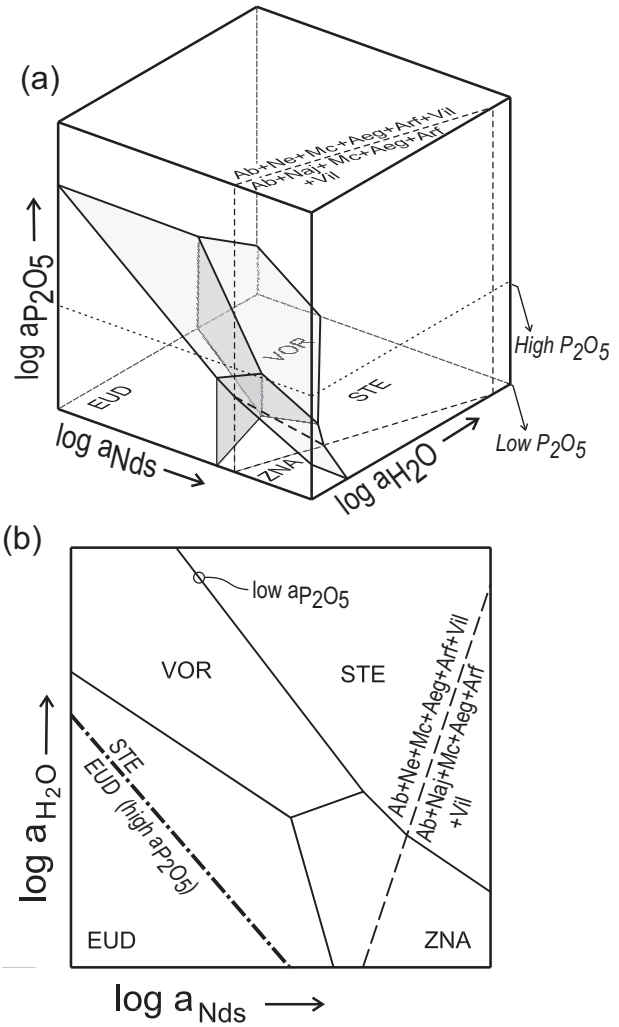

Fig. 7. Part of a grid for Zr-rich minerals in log a_{Nds}–log a_{H2O}–log a_{P2O5} space for a system saturated in Ab + Mc + Arf + Aeg + Vil and straddling the Ne–Naj boundary in Fig. 6. (a) A 3D rendering showing stability fields for eudialyte (Eud), voronkovite (Vor), zirsinalite (Zna) and steenstrupine-(Ce) (Ste) in the presence of silicate melt, albite, nepheline or naujakasite, arfvedsonite, aegirine, sodalite and villiaumite. Compositions of eudialyte and voronkovite used are given in Table 1. Because voronkovite has not been observed to coexist with naujakasite, whereas there is indirect evidence that zirsinalite has, the plane representing Vor + Zna coexistence has been placed outside the naujakasite volume in the diagram. High P_2O_5 and Low P_2O_5 indicate the positions of high- and low-a_{P2O5} sections shown in (b). (b) Sections at constant a_{P2O5} through the grid in (a). The low-a_{P2O5} section represents the base of the 3D grid; the high-a_{P2O5} section is above the point of Vor + Eud + Zna + Ste coexistence.

high a_{HF} [reaction (d3)], close to the fluorite-saturation surface; at increasing a_{Nds}, the hiortdahlite field is truncated by stable eudialyte + fluorite. At high a_{Nds}, the eudialyte field is limited by the steenstrupine-(Ce)-in reaction [reactions (d4a) and (d4b)], which is independent of a_{HF}, but dependent on phosphorus (P_2O_5) activity, and therefore not a real divariant reaction in the system. At increasing a_{P2O5}, the steenstrupine-in surface is displaced towards lower a_{Nds} (Fig. 7). The prevalence of steenstrupine-(Ce)-bearing mineral assemblages in hyperagpaitic rocks suggests that the scenario indicated in Fig. 6, which corresponds to a relatively elevated P_2O_5 activity, is the most relevant estimate of the stability relationships in Ilímaussaq. However, at lower P_2O_5 activity stability volumes for voronkovite and zirsinalite appear at high a_{Nds} (and high and low a_{H2O}, respectively; Fig. 7). Because eudialyte does not appear to coexist with naujakasite in Ilímaussaq, but there is indirect evidence that zirsinalite does, the Vor–Zna coexistence plane [reaction (e3)] has been drawn at the low a_{Nds} side of the naujakasite-in plane in Fig. 7.

The naujakasite + eudialyte + albite + microcline + arfvedsonite assemblage is in principle stable at high a_{Nds} and low a_{H2O} (Fig. 6). The lack of coexisting eudialyte and naujakasite in Ilímaussaq suggests that such conditions have not been attained, and that water activity lower than that corresponding to the intersection of the Ab + Ne + Mc + Naj and Eud + Ste planes in Fig. 6 is not relevant for naujakasite lujavrite in Ilímaussaq.

Titanium minerals

In most lujavrite varieties, TiO_2 contents are low (Bailey *et al.*, 2001, 2006) and titanium tends to be camouflaged

in the main rock-forming minerals (amphibole, pyroxene, magnetite). This is reflected by a large Ti-undersaturated volume in the petrogenetic grid in Fig. 8. This volume is bordered by volumes for aenigmatite at low a_{Nds} and a_{H2O}, for astrophyllite at high a_{H2O} and low a_{Nds}, and for rinkite at elevated a_{HF}. The lower boundary of the rinkite volume [rinkite-in reaction, (f5)] parallels the villiaumite saturation plane. Because rinkite has essential Ca, low a_{CaO} may reduce the size of the stability volume of rinkite by shifting its lower boundary to higher a_{HF}, or suppress it completely.

In phosphorus-rich systems, the high a_{Nds} part of the grid is occupied by a stability volume for vuonnemite, whose boundary towards low a_{Nds} [reactions (f3a) and (f3b)] is dependent on both P_2O_5 and Nb_2O_5 activities. At lower a_{P2O5}, the vuonnemite-in plane is displaced towards higher a_{Nds}. Several Na–Ti silicate minerals are possible hosts for Ti in low-phosphorus systems (Table 1); among these, only epistolite appears to be a realistic alternative in Ilímaussaq (Karup-Møller, 1986*b*). The stability field of epistolite is limited by reaction (f4), and is situated at high a_{H2O} and a_{Nds} (Fig. 8a).

Alkali phosphate minerals

The mineral assemblage with arfvedsonite, sodalite, ussingite, villiaumite, vitusite-(Ce) [$Na_3REE(PO_4)_2$], natrophosphate [$Na_7(PO_4)_2F{\cdot}19H_2O$] and vuonnemite illustrated in Fig. 2d may represent a near endpoint of hyperagpaitic magmatic evolution in Ilímaussaq. The stability of vitusite-(Ce) and natrophosphate is independent of the HFSE-bearing minerals in the system, but depends on the P_2O_5 and [for vitusite-(Ce)] REE_2O_3 activities. A schematic illustration of the stability relationship of these phosphate minerals in the presence of steenstrupine-(Ce), vuonnemite, ussingite, villiaumite and sodalite is illustrated in Fig. 9. Natrophosphate and vitusite-(Ce) are stable at elevated a_{H2O} and a_{Nds}. There are different reactions linking these minerals to more common P- and REE-hosting phases such as apatite and monazite, or to systems undersaturated in phosphorus and REE (Table 3). The orientation of formally univariant lines for reactions involving apatite and monazite are, however, identical or closely similar to those involving REE_2O_3 and P_2O_5 components in the melt in log activity space. Coexisting vitusite-(Ce) and natrophosphate are stable together at conditions that approach natrosilite saturation.

DISCUSSION

Magmatic evolution and agpaitic mineral assemblages

It is generally accepted that the highly alkaline magmas that formed the Ilímaussaq complex were the ultimate products of extensive fractional crystallization of an alkali basaltic parent magma. The immediate precursors of the agpaitic magmas in the complex may be similar in composition to the augite syenite of the border group

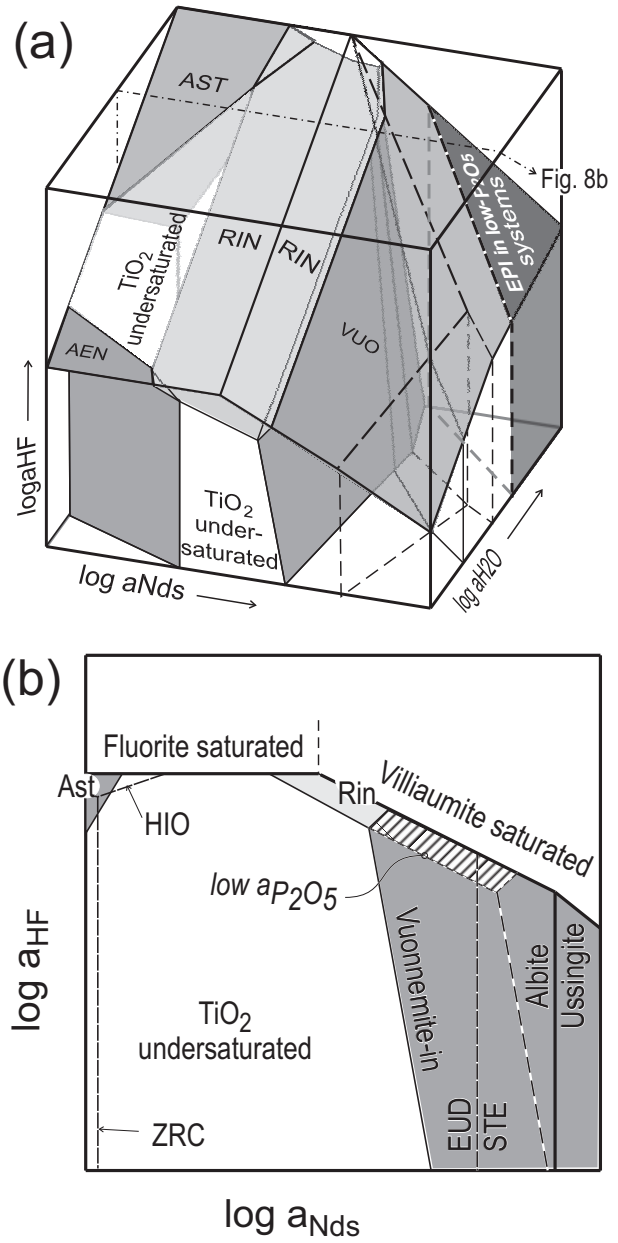

Fig. 8. (a) A 3D rendering of the stability fields of titanium minerals in log a_{Nds}–log a_{H2O}–log a_{HF} space in the presence of albite or ussingite, nepheline or naujakasite, arfvedsonite, sodalite and silicate melt, compatible with the grids in Figs 5 and 6. The divariant reactions illustrated are listed in Table 3. Stability volumes have been constructed for aenigmatite (Aen), vuonnemite (Vuo), astrophyllite (Ast) and rinkite (Rin). These volumes surround a large, TiO_2-undersaturated central volume in which Ti is camouflaged in other rock-forming minerals. (b) log a_{Nds}–log a_{HF} section through the 3D grid in (a), showing stability fields of astrophyllite (Ast), rinkite (Rin) and vuonnemite (Vuo). Stability fields for zircon, hiortdahlite, eudialyte, steenstrupine-(Ce), albite and ussingite from Figs 5 and 6 are shown for comparison (upper case abbreviations identify stability fields of the Zr-minerals). The stability of vuonnemite is dependent on P_2O_5 activity, and the vuonnemite-in line will shift to higher a_{Nds} at lower a_{P2O5}. As a consequence, the rinkite field will also expand towards higher a_{Nds} (ruled field). The low P_2O_5 scenario is indicated by dashed lines superimposed on the high-a_{P2O5} vuonnemite field.

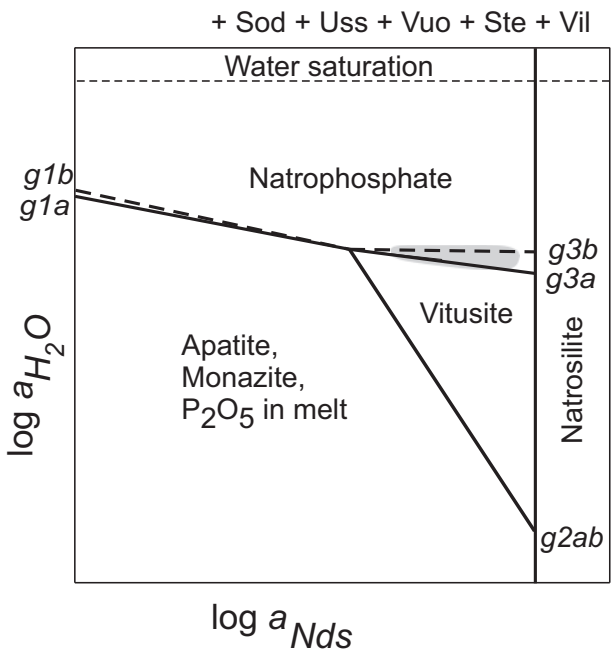

Fig. 9. Sketch of a stability diagram for phosphate minerals at highly hyperagpaitic conditions, assuming the presence of a silicate melt. The shaded field represents the phase relationships illustrated in Fig. 2d; further evolution along the natrophosphate–vitusite-(Ce) line will lead to saturation in natrosilite. Lines are labeled with reaction numbers from Table 3.

or to a microkakortokite dyke exposed outside the intrusion (Larsen & Steenfeldt, 1974; Marks & Markl, 2003). It has been suggested that more than 90% of the original magma crystallized before the agpaitic stage was reached, and significantly higher degrees of fractionation are needed to account for hyperagpaitic residual melts (Upton, 2014, and references therein). It is also generally assumed that fractionation took place in a closed system, either *in situ* or at some deeper level in the crust (Ferguson, 1970; Engell, 1973; Sørensen & Larsen, 2001; Sørensen *et al.*, 2011). In a closed total system, the contents of volatile components not incorporated into the fractionating solids will increase in the residual melt.

The sequence of increasingly peralkaline agpaitic rock compositions from sodalite foyaite through kakortokite, and naujaite to lujavrite is coupled to a change in magmatic mineralogy compatible with increasing a_{Nds} from zircon- or hiortdahlite-, through eudialyte + fluorite-, eudialyte + villiaumite-, to steenstrupine-(Ce) ± vuonnemite- or voronkovite-bearing assemblages (Figs 6 and 7). Eventually, minerals such as ussingite and naujakasite were stabilized, and assemblages with alkali phosphate minerals and natrosilite represent the final products of the fractionation trend (Figs 6 and 9). The low-alkali stage of this evolution, characterized by hiortdahlite-bearing assemblages, is a stage of evolving peralkaline magmas similar to that seen in the Langesundsfjord suite of nepheline syenite pegmatites in the Oslo Rift, Norway (Andersen *et al.*, 2010, 2013). In the Oslo Rift pegmatites, shifts in water and HF activity were as important for the evolution toward agpaitic conditions as increasing peralkalinity. In Ilímaussaq, the scarcity of primary hydrated Ti- and Zr-silicates (i.e. astrophyllite, catapleiite and rinkite), which are typical in alkaline complexes such as the Larvik plutonic complex, indicates that excursions towards high water activity at low a_{Nds} were not important during the main agpaitic phase of magmatic evolution. The presence of rinkite and magmatic fluorite in kakortokite, naujaite and some lujavrites indicates a high level of a_{HF} throughout the main phase magmatic crystallization, and therefore no changes in magmatic mineralogy can be attributed to shifts in a_{HF} prior to the hyperagpaitic stage of evolution of the magma.

The agpaitic–hyperagpaitic boundary and the role of villiaumite

The transition from agpaitic to hyperagpaitic conditions is marked by the appearance of characteristic indicator minerals including minerals of relatively simple composition such as villiaumite, ussingite and naujakasite, and highly alkaline HFSE silicate or phosphosilicate minerals [steenstrupine-(Ce), vuonnemite, voronkovite, zirsinalite and others]. Villiaumite is commonly the first hyperagpaitic indicator mineral to appear (Rose-Hansen & Sørensen, 2002), and it is therefore important to understand its role in the crystallization history of agpaitic magmas. Magmatic villiaumite will start to crystallize when a fluorite-saturated, fractionating magma intersects the boundary between the fluorite and villiaumite fields in the grid in Fig. 6, or when the line of evolution of a magma that was initially undersaturated in fluoride minerals penetrates the sloping villiaumite saturation surface from below at higher a_{Nds}. In the system considered here, the villiaumite saturation surface is a nominally divariant plane, tied to the main rock-forming mineral assemblages through phase equilibria (Table 3). However, because of the unconstrained calcium activity in the Ilímaussaq lujavrite, the boundary between the fluorite and villiaumite fields is not equally well constrained, and the HF activity level of fluorite saturation depends on CaO activity; low a_{CaO} moving the fluoride saturation plane to higher a_{HF}, but at the same time shifting the boundary between fluorite and villiaumite towards lower a_{Nds} (Fig. 6).

As long as the a_{HCl} and the Zr content of the melt remain sufficiently high to stabilize eudialyte, this mineral has a very wide stability field in log a_{Nds}–log a_{H2O}–log a_{HF} space, which extends to higher a_{Nds} than reasonable estimates of the fluorite–villiaumite boundary (Fig. 6). At a_{Nds} within the stability volume of eudialyte, but below the villiaumite-saturation plane, a silica-undersaturated, highly peralkaline silicate melt will crystallize albite, nepheline, microcline, arfvedsonite, eudialyte ± sodalite; that is, the major minerals of kakortokite, naujaite and most lujavrite in Ilímaussaq, which is an agpaitic rather than a hyperagpaitic mineral

assemblage (point × in Fig. 10). Such a magma would have a highly elevated (Na + K)/Al ratio, but it would crystallize an agpaitic rather than a hyperagpaitic mineral assemblage. If the activity parameters are kept constant, the end product of crystallization will be a lujavrite or kakortokite with a normal agpaitic mineral assemblage, or a naujaite, if the activity of HCl is sufficiently high to stabilize sodalite as a magmatic mineral. Because of the slope of the villiaumite saturation surface, several lines of liquid evolution may lead to saturation of the magma in villiaumite. This includes an increase in a_{Nds} at constant a_{H2O} and a_{HF} (path 1), simultaneous increases in a_{Nds} and a_{HF} (path 2), in a_{HF} only (path3), and even an increase in a_{HF} at decreasing a_{Nds} (path 4). A decrease in a_{Nds} could be more dramatic than illustrated in Fig. 10, because the line of fluorite + villiaumite coexistence will recede towards lower a_{Nds} at decreasing a_{CaO}. Depending on the HF activity of the starting point, even a decrease of a_{H2O} at constant (path 5) or decreasing a_{HF} may cause crystallization of villiaumite. The presence of villiaumite as the sole hyperagpaitic indicator mineral in a rock is therefore not evidence that a magma has evolved towards increasing peralkalinity (or increasing a_{Nds}).

Effects of peralkalinity and water activity

Increasing peralkalinity or at least a high a_{Nds} is in general needed to stabilize other characteristic minerals of hyperagpaitic rocks, such as ussingite, naujakasite, steenstrupine-(Ce), voronkovite and natrosilite. The orientation of the ussingite-in and steenstrupine-(Ce)-in boundaries is such that an increase in water activity, with or without a concomitant increase in peralkalinity, may force hyperagpaitic mineral assemblages with ussingite and steenstrupine-(Ce) to form at the expense of eudialyte + albite (Fig. 6; path 6 in Fig. 10). If the starting point is sufficiently close to the naujakasite-in plane, and a_{HF} is so low that a reduction in a_{H2O} will not force the melt to intersect the villiaumite saturation plane, falling a_{H2O} may in principle provoke crystallization of naujakasite (Figs 5a and 6). However, this type of evolution is considered unrealistic for Ilímaussaq: the absence of coexisting naujakasite and eudialyte in hyperagpaitic lujavrite suggests that the intersection of the steenstrupine-(Ce)-in and naujakasite-in planes in Fig. 6 defines a minimum limit of water activity for magmatic crystallization in Ilímaussaq (shown as a dash–dot line in Fig. 6). Any melt that could potentially be forced to crystallize naujakasite by reduction of the water activity would have to start at higher water activity than this limit, which would lie within the steenstrupine-(Ce) stability field; that is, the magma would already be defined as hyperagpaitic by indicator minerals other than naujakasite.

One interesting possibility that arises from the scenario illustrated by paths 5 and 6 in Fig. 10 is that loss of an aqueous fluid phase from a magma crystallizing a 'normal' agpaitic magmatic mineral assemblage may force the dehydrated silicate melt to crystallize villiaumite; that is, to become hyperagpaitic by dehydration (path 5). Simultaneously, an aqueous fluid expelled into already solidified lujavrite or into the wall-rocks may cause crystallization of high-water hyperagpaitic

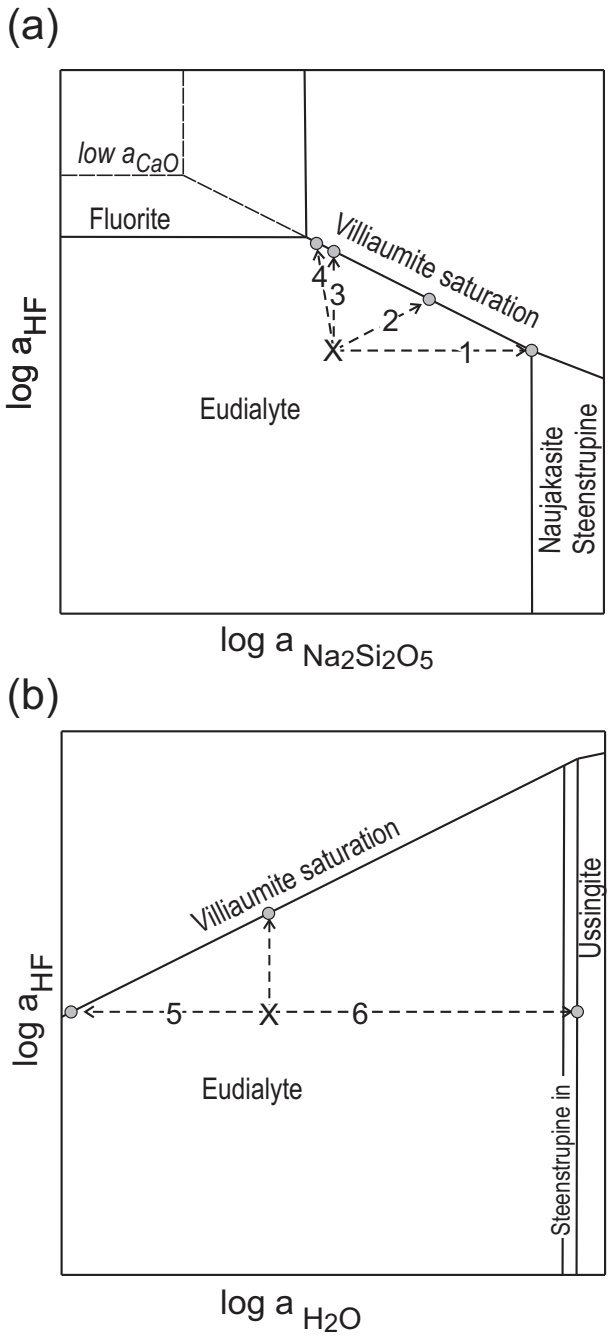

Fig. 10. Sections at constant a_{H2O} (a) and constant a_{Nds} (b) through the high-a_{Nds} part of the eudialyte stability field in Fig. 6. Point × represents an agpaitic silicate melt crystallizing albite + nepheline + arfvedsonite + eudialyte + sodalite; that is, a magmatic assemblage corresponding to agpaitic rocks such as sodalite foyaite, naujaite or kakortokite. Six evolutionary trends leading to the crystallization of hyperagpaitic mineral assemblages from residual melts are shown (numbered 1–6). Of these, only two (1 and 2) require a net increase in a_{Nds}. (See discussion in the text.)

mineral assemblages with ussingite, steenstrupine-(Ce) ± vuonnemite (path 6). In such a hypothetical case, hyperagpaitic crystallization conditions are caused by separation of a free fluid, followed by migration of the fluid and not by increase in peralkalinity or fluorine content of the residual magma. Two very different hyperagpaitic mineral assemblages (villiaumite- and ussingite-bearing, respectively) may form as a result of a single process. Fluid inclusions in minerals in late-magmatic veins with ussingite and other characteristic hyperagpaitic minerals comprise alkali chloride brine and hydrocarbons, which were immiscible at the time of trapping (Konnerup-Madsen, 2001, and references therein; Krumrei *et al.*, 2007; Graser, 2008). During separation of such fluid, fluorine would in general be partitioned into the coexisting silicate melt (Carroll & Webster, 1994), which is supported by analyses of extracted inclusion fluids from Ilímaussaq suggesting F/Cl ratios by weight in the range 2×10^{-1} to 4×10^{-4} (Graser, 2008). Separation of a saline aqueous fluid from lujavrite magma, followed by migration and fluid–rock interaction, may account for post-magmatic veins and metasomatic zones with high-water hyperagpaitic mineralogy; the petrogenesis of these is, however, beyond the scope of this study.

Fractional crystallization vs open-system processes

Most of the agpaitic igneous rocks in the Ilímaussaq alkaline complex are cumulates whose compositions differ from that of the magmas from which they crystallized. In contrast to pegmatites, veins and metasomatic zones in the wall-rocks, naujakasite lujavrite is a genuine magmatic rock that represents the end-product of differentiation in this system, and that must have formed at highly elevated a_{Nds}. Naujakasite has a narrow stability field in log a_{Nds}–log a_{H2O}–log f_{O2} space, and for a peralkaline magma to reach a stage of evolution where naujakasite can crystallize, the liquid line of descent must be able to penetrate the nepheline–albite–aegirine plane, which is a potential thermal divide in the simplified lujavrite system Si–Al–Na–Fe–O–H (Andersen & Sørensen, 2005). This requires a special combination of low oxygen fugacity and elevated water activity at a stage of evolution prior to naujakasite crystallization, which may be the main reason why naujakasite is such a rare mineral, even in highly peralkaline rocks. In a more complex chemical system (e.g. the 15-component system used in this study), other factors will also combine to prevent a magma from reaching compositions where naujakasite and other hyperagpaitic indicator minerals will be able to crystallize. The kakortokite and microkakortokite of Ilímaussaq plot well within the Ab–Ne–Arf–Aeg volume in the $NaO_{0.5}$–$AlO_{1.5}$–SiO_2–FeO_{tot} tetrahedron (Fig. 11). Both eudialyte and sodalite fall outside this volume, on the high-alkali side of the Ab–Ne–Aeg plane [represented by a bold line in the $Fe_{tot}/(Na+K)$ vs $Al/(Na+K)$ diagram in Fig. 11b].

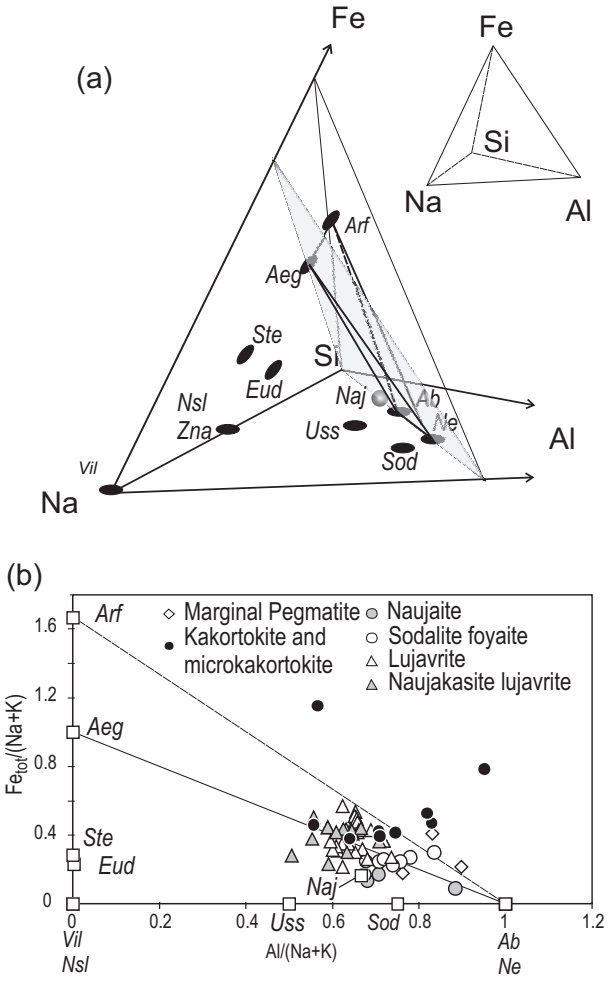

Fig. 11. (a) A 3D view of the $NaO_{0.5}$–$AlO_{1.5}$–SiO_2–FeO^t tetrahedron, showing the compositions of minerals in the agpaitic nepheline syenite in Ilímaussaq (e.g. Engell, 1973; Andersen & Sørensen, 2005). The Ab–Ne–Aeg plane is shown by shading, and the Ab–Ne–Aeg–Arf volume by a bold outline. Ab, albite; Ne, nepheline; Sod, sodalite; Uss, ussingite; Naj, naujakasite; Eud, eudialyte; Nsl, natrosilite; Zna, zirsinalite; Vil, villiaumite; Ste, steenstrupine-(Ce); Arf, arfvedsonite; Aeg, aegirine. Ne, Ab, Sod, Nsl and Vil plot in the Na–Al–Si (bottom) plane of the diagram, and Eud, Ste, Arf and Aeg in the Na–Si–Fe plane, only Naj falling within the volume of the tetrahedron. (b) Minerals (squares) and analyzed whole-rocks shown in an element ratio diagram $Fe_{tot}/(Na+K)$ vs $Al/(Na+K)$. $Al/(Na+K)$ rather than the more conventional $(Na+K)/Al$ has been chosen to avoid divisions by zero. The Ab–Ne–Aeg–Arf volume in (a) is represented by the area between the (Ab,Ne)–Aeg and (Ab,Ne)–Arf lines in the diagram. The potential thermal divide along the Ab–Ne–Aeg plane represented by the solid line must be penetrated by magmas evolving towards hyperagpaitic residual liquids, as discussed by Andersen & Sørensen (2005). (See further discussion in the text.) Sources of rock analyses: Ussing (1912); Engell (1973); Larsen & Steenfeldt (1974); Sørensen (1997, 2006); Bailey *et al.* (2001, 2006); Khomyakov *et al.* (2001). Kakortokite and microkakortokite samples plotting at the low-alkali side of the projection of the Ne–Ab–Arf plane are samples that have lost alkalis during crystallization (Larsen & Steenfeldt, 1974).

Fractionation of either or both of these minerals with albite, nepheline and arfvedsonite from a normal agpaitic magma will therefore be an even more effective mechanism to drive residual liquids away from the

Aeg–Ab–Ne plane, and thereby prevent formation of hyperagpaitic residual liquids, than is fractionation of aegirine. The magma(s) forming the main series of kakortokite floor cumulates and the naujaite roof cumulates will have fractionated massive amounts of eudialyte and/or sodalite, and are therefore unlikely to penetrate the Ab–Ne–Aeg plane, unless assisted by other factors. One such factor may be depletion of the agpaitic residual magma in zirconium and chlorine. These elements are essential for eudialyte (Zr, Cl) and sodalite (Cl), and are thus also highly compatible during fractionation of those minerals. Removal of sufficient amounts of Zr and Cl by fractional crystallization of eudialyte ± sodalite may destabilize these minerals in the residual melt, and thus allow fractional crystallization trends to turn towards hyperagpaitic residual liquids. It should be noted that hyperagpaitic lujavrite is commonly lower in chlorine than other agpaitic rock types in Ilímaussaq (Bailey *et al.*, 2001, 2006; Sørensen, 1997).

Because the composition of sodalite falls to the high-Na side of the Ab–Ne–Aeg plane, sodalite-rich cumulates (sodalite foyaite, naujaite) also plot outside the Ab–Ne–Arf–Aeg volume without being hyperagpaitic (Fig. 11); the excess Na in these rocks will be bound in sodalite, and thus not be available to form naujakasite or other hyperagpaitic minerals. However, interaction of sodalite-rich cumulate rocks with a chlorine-depleted, sodalite-undersaturated lujavrite magma may cause reaction (b1) in Table 3 to run from right to left, resorbing sodalite, increasing the peralkalinity of the melt and, possibly, forcing the formation of naujakasite by reaction (a2). Interaction between solid naujaite and lujavrite magma has indeed taken place in the intrusion (Rose-Hansen & Sørensen, 2002). Figure 3b shows a sodalite crystal that has been resorbed and rimmed by albite, as would be expected from reaction (b1). If selective resorption of sodalite into a low-a_{HCl} lujavrite magma was part of this process, the affected magma could become hyperagpaitic by intraplutonic assimilation. The concentration of the naujakasite lujavrite intrusions in the upper part of the sandwich horizon and along the upper, northern boundary of the intrusion has generally been taken as evidence for increasing degrees of closed-system fractionation. It would, however, be equally compatible with a selective assimilation process, as the late intrusions in those parts of the complex are also those that would have the highest probability of interacting with naujaite.

The diverse paths to hyperagpaicity

It follows from the above discussion that not only are there different kinds of hyperagpaitic rocks in the Ilímaussaq complex, but agpaitic precursors may evolve to hyperagpaitic residual liquids by different lines of descent, depending upon initial composition and the conditions under which they crystallize. The most important paths to hyperagpaicity are summarized in a qualitative flow chart in Fig. 12.

An agpaitic precursor magma crystallizing alkali feldspar, nepheline and arfvedsonite (represented by the central, shaded box in Fig. 12) situated at the low-alkali side of the Ab–Ne–Aeg plane in Fig. 11a will evolve to a less alkaline (but still agpaitic) residual composition, if high-alkali minerals (aegirine, eudialyte or sodalite) join the crystallizing assemblage. This critical plane (and the corresponding Ab–Ne–Eud plane) may be penetrated only if early crystallization of the high-alkali minerals is suppressed, or possibly by assimilation of sodalite. Once past the Ab–Ne–Eud barrier, residual liquids will be driven towards more alkaline residuals, even by crystallization of assemblages including eudialyte. Three groups of paths towards hyperagpaicity may be envisaged, as follows.

1. Fractionation of Ab + Ne + Arf + Eud may occur until the residual liquid encounters the steenstrupine-in reaction (d4a) or, in the case of low-phosphorus systems, the eudialyte–voronkovite reaction (e1). At low to moderate initial water content, such liquids will evolve towards villiaumite saturation and the naujakasite-in reaction (a2) to form naujakasite lujavrite. At higher water content, they may instead encounter the ussingite-in reaction (a1).
2. Melts with high water content may, regardless of eudialyte crystallization, intersect the albite–nepheline–analcime plane (Fig. 5b) before reaching hyperagpaitic compositions, and possibly develop from there to ussingite-bearing final assemblages, examples of which are seen in hydrothermal veins (Markl & Baumgartner, 2002).
3. The third group of liquid lines of descent starts at lower water content, and intersects the villiaumite-in plane before any of the other characteristic reactions are encountered. Such liquids may continue evolving through the eudialyte–steenstrupine and nepheline–naujakasite reactions to end up as naujakasite lujavrite, or they may end with a final assemblage Ab + Ne + Arf + Eud + Vil; that is, as a villiaumite lujavrite straddling the boundary between the agpaitic and hyperagpaitic realms. Villiaumite lujavrite assemblages will also result if an aqueous fluid is lost from a melt crystallizing Ab + Ne + Arf + Eud.

CONCLUSIONS

Hyperagpaitic rocks in the Ilímaussaq alkaline complex include both true magmatic intrusions of villiaumite and naujakasite lujavrite, pegmatites, late-magmatic veins and alteration zones in the wall-rocks. Each of these has specific assemblages of hyperagpaitic minerals. From a chemographic analysis of low-variance agpaitic and hyperagpaitic magmatic mineral assemblages in hyperagpaitic lujavrite in the simplified system $NaO_{0.5}$–$KO_{0.5}$–CaO–FeO–$FeO_{1.5}$–$REEO_{1.5}$–ZrO_2–TiO_2–$NbO_{2.5}$–$PO_{2.5}$–$AlO_{1.5}$–SiO_2–$HO_{0.5}$–$FO_{-0.5}$–$ClO_{-0.5}$ these can be related to distinct combinations of peralkalinity (represented by a_{Nds}; i.e. the activity of the

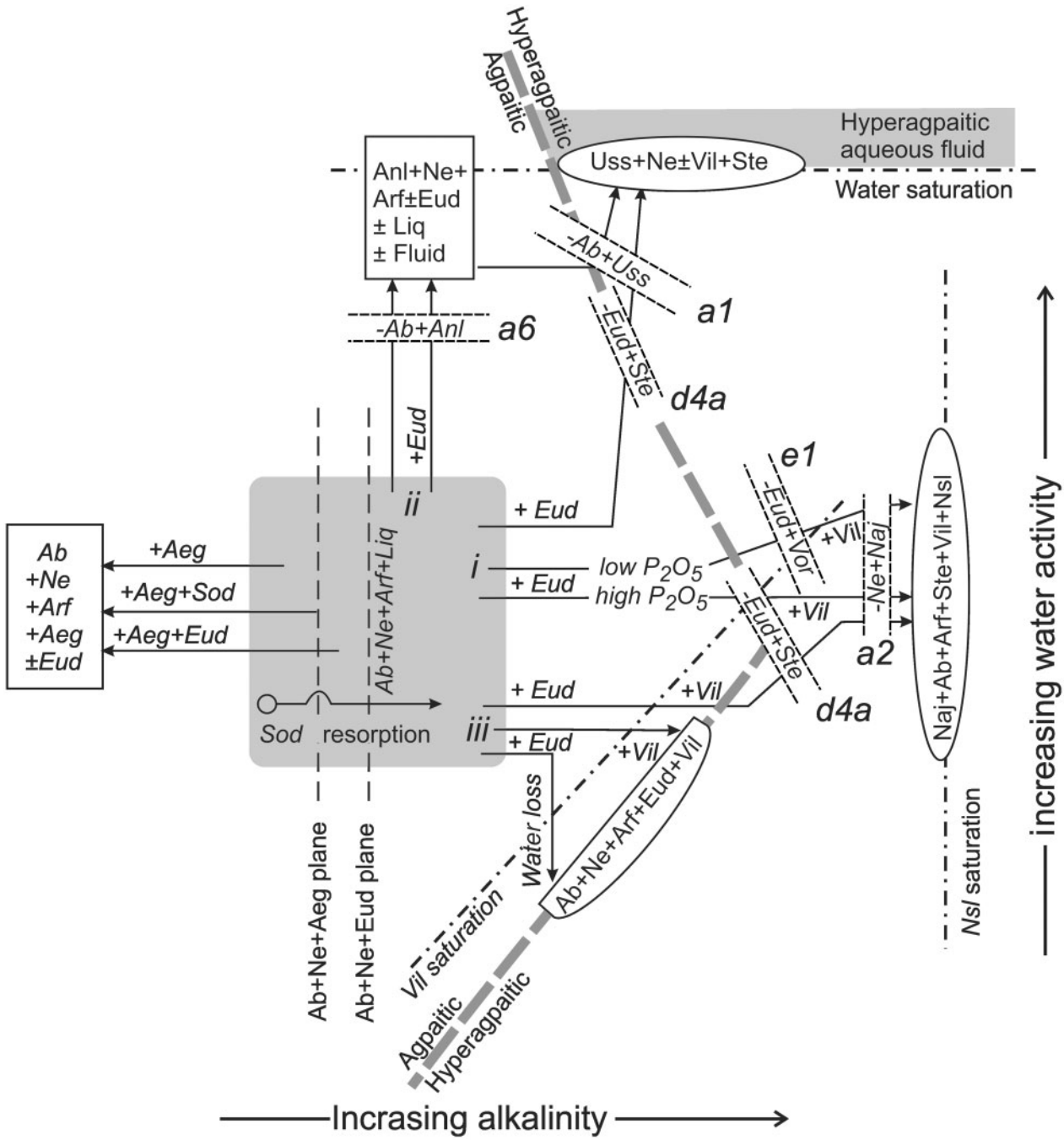

Fig. 12. Flow-chart in qualitative alkalinity–water activity space summarizing the liquid lines of evolution from agpaitic to hyperagpaitic conditions. The central, shaded field represents agpaitic magmas that crystallize alkali feldspar, nepheline and arfvedsonite. Liquid lines of descent driven by crystallization of these minerals and additional minerals as indicated are shown as arrows; the critical planes Ab + Ne + Aeg (see Fig. 11) and Ab + Ne + Eud are shown by dashed lines. The thick, dashed, grey curve represents the approximate boundary between the agpaitic and hyperagpaitic realms. Rectangles represent the final solid assemblages (i.e. rocks) of agpaitic mineralogical character; ellipses represent hyperagpaitic rocks. Rocks having villiaumite as the only indicator mineral may not be truly hyperagpaitic (see discussion in the text), and the field surrounding the Ab + Ne + Arf + Eud + Vil solid assemblage is therefore shown straddling the boundary with partly angular, partly rounded edges. Double dashed lines crossing the evolution paths represent changes in solid assemblage or reaction relationships, identified by – (phase out),+(phase in) and reaction numbers referring to Table 3. Saturation with villiaumite, natrosilite and water is shown by dash–dot lines. Numerals i, ii and iii represent the three main groups of liquid lines of descent that may lead to hyperagpaitic final residuals.

$Na_2Si_2O_5$ component), water, halogen and phosphorus activities.

The main trend of agpaitic magma evolution, from sodalite foyaite and microkakortokite through kakortokite and naujaite cumulate formation to arfvedsonite lujavrite magma, involves steadily increasing a_{Nds}, at relatively high a_{HF} (at or close to fluorite and/or villiaumite saturation) and a_{HCl} at the sodalite saturation

limit. This pattern changes once the magma has reached a potentially hyperagpaitic level of $Na_2Si_2O_5$ enrichment. Over a large volume of a_{Nds}–a_{H2O}–a_{HF} space a highly peralkaline magma that crystallizes albite + microcline + nepheline + sodalite + arfvedsonite + eudialyte may change into crystallizing villiaumite (i.e. become hyperagpaitic) by an increase in a_{HF} relative to the inclined villiaumite-saturation plane without simultaneous change in a_{Nds} (or even at decreasing a_{Nds}). Crystallization of naujakasite, steenstrupine-(Ce) and natrosilite is, however, a strong indication of increasing peralkalinity. In contrast, ussingite is an indicator of elevated water activity, and an aqueous fluid expelled from an ordinary agpaitic magma may form mineral assemblages with ussingite in late-magmatic veins within the intrusion and metasomatized domains in the wall-rocks ('fenite'). Simultaneously, a dehydrated agpaitic magma may be forced into crystallization of villiaumite, so that saturation and migration of an aqueous fluid from a single agpaitic magma may cause the formation of hyperagpaitic rocks with contrasting high-water (ussingite) and low-water (villiaumite) indicator mineral assemblages.

Separation of eudialyte and sodalite, as seen in kakortokite and naujaite, prevents residual liquids from reaching hyperagpaitic compositions by closed-system fractional crystallization. An alternative way for a lujavrite magma to acquire a hyperagpaitic composition is by intraplutonic assimilation of sodalite (e.g. from naujaite cumulate), provided that the HCl activity of the lujavrite magma is below the saturation limit for sodalite at the time of interaction with naujaite.

ACKNOWLEDGEMENTS

This paper is dedicated to the memory of Professor Henning Sørensen, Copenhagen University (1926–2013), whose long and distinguished career was dedicated to the understanding of agpaitic and hyperagpaitic rocks. Greenland Minerals and Energy Ltd is thanked for making core samples available and for funding H.F. Thanks are due to Lotte Melchior Larsen and Adrian Finch for helpful discussions and advice, and to Irina Papenberg for acquiring the macro photograph of the drill core. Special thanks go to Ray Macdonald, Michael Marks and Adrian Finch for helpful reviews.

FUNDING

This study has received support from the University of Oslo through a Småforsk grant from the Department of Geosciences to T.A.

SUPPLEMENTARY DATA

Supplementary data for this paper are available at *Journal of Petrology* online.

REFERENCES

Allaart, J. H. (1973). *Geological Map of Greenland 1:100000, Julianehåb 60V.2 Nord*. Copenhagen: Grønlands Geologiske Undersøgelse.

Andersen, T. & Sørensen, H. (2005). Stability of naujakasite in hyperagpaitic melts, and the petrology of naujakasite lujavrite in the Ilímaussaq alkaline complex, South Greenland. *Mineralogical Magazine* **69**, 125–136.

Andersen, T., Erambert, M., Larsen, A. O. & Selbekk, R. S. (2010). Petrology of nepheline syenite pegmatites in the Oslo Rift, Norway: Zirconium silicate mineral assemblages as indicators of alkalinity and volatile fugacity in mildly agpaitic magma. *Journal of Petrology* **51**, 2303–2325.

Andersen, T., Erambert, M., Selbekk, R. S. & Larsen, A. O. (2013). Petrology of nepheline syenite pegmatites in the Oslo Rift, Norway: Zr and Ti mineral assemblages in miaskitic and agpaitic pegmatites in the Larvik Plutonic Complex. *Mineralogia* **44**, 61–98.

Bailey, J. C., Bohse, H., Gwozdz, R. & Rose-Hansen, J. (1993). Li in minerals from the Ilímaussaq alkaline intrusion, South Greenland. *Bulletin of the Geological Society of Denmark* **40**, 288–299.

Bailey, J. C., Gwozdz, R., Rose-Hansen, J. & Sørensen, H. (2001). Geochemical overview of the Ilímaussaq alkaline complex, South Greenland. In: Sørensen, H. (ed.) *The Ilímaussaq alkaline complex, South Greenland: status of mineralogical research with new results. Geology of Greenland Survey Bulletin* **190**, 35–53.

Bailey, J. C., Sørensen, H., Andersen, T., Kogarko, L. N. & Rose-Hansen, H. (2006). On the origin of microrhythmic layering in arfvedsonite lujavrite from the Ilímaussaq alkaline complex, South Greenland. *Lithos* **91**, 301–318.

Bellezza, M., Merlino, S. & Perchiazzi, N. (2009a). Mosandrite: Structural and crystal-chemical relationships with rinkite. *Canadian Mineralogist* **47**, 897–908.

Bellezza, M., Merlino, S., Perchiazzi, N. & Raade, G. (2009b). 'Johnstrupite': A chemical and structural study. *Atti della Società Toscana di Science Naturali, Serie A* **114**, 1–3.

Bondam, J. & Ferguson, J. (1962). *An occurrence of villiaumite in the Ilímaussaq intrusion, South Greenland. Meddelelser om Grønland* **172**(**2**), 13 pp.

Brøgger, W. C. (1890). Die Mineralien der Syenitpegmatitgänge der südnorwegischen Augit- und Nephelinsyenite. *Zeitschrift für Krystallographie* **16**, 1–235 (part 1) + 1–663 (part 2).

Camara, F., Sokolova, E. & Hawthorne, F. C. (2011). From structure topology to chemical composition. XII. Titanium silicates: the crystal chemistry of rinkite $Na_2Ca_4REETi(Si_2O7)OF_3$. *Mineralogical Magazine* **75**, 2755–2774.

Carroll, M. R. & Webster, J. D. (1994). Solubilities of sulfur, noble gases, nitrogen, chlorine and fluorine in magmas. In: Carroll, M. R. & Holloway, J. R. (eds) *Volatiles in Magmas. Mineralogical Society of America, Reviews in Mineralogy* **30**, 231–279.

Chakmouradian, A. R. & Zaitsev, A. N. (2012). Rare earth mineralization in igneous rocks: Sources and processes. *Elements* **8**, 347–353.

Danø, M. & Sørensen, H. (1959). *An examination of some rare minerals from the nepheline syenites of South West Greenland. Grønlands Geologiske Undersøgelse Bulletin* **20**, 35 pp.

Engell, J. (1973). A closed system crystal fractionation model for the agpaitic Ilímaussaq intrusion, South Greenland with special reference to the lujavrites. *Bulletin of the Geological Society of Denmark* **22**, 334–362.

Ercit, T. S., Cooper, M. A. & Hawthorne, F. C. (1998). The crystal structure of vuonnemite, $Na_{11}TiNb_2(Si_2O_7)_2(PO_4)_2O_3(F,OH)$,

a phosphate-bearing sorosilicate of the lomonosovite group. *Canadian Mineralogist* **36**, 1311–1320.

Ferguson, J. (1964). *Geology of the Ilímaussaq alkaline intrusion, South Greenland. Description of map and structure. Meddelelser om Grønland* **172**(**4**), 82 pp.

Ferguson, J. (1970). *The significance of the kakortokite in the evolution of the Ilímaussaq intrusion, South Greenland. Grønlands Geologiske Undersøgelse Bulletin* **89**, 193 pp.

Graser, G. (2008). Late-magmatic to hydrothermal processes in the Ilímaussaq intrusion, South Greenland. Dissertation zur Erlangung des Grades eines Doktors der Naturwissenschaften der Geowissenschaftlichen Fakultät der Eberhard-Karls-Universität Tübingen, 81 pp.

Hettmann, K., Wenzel, T., Marks, M. & Markl, G. (2012). The sulfur speciation in S-bearing minerals: New constraints by a combination of electron microprobe analysis and DFT calculations with special reference to sodalite-group minerals. *American Mineralogist* **97**, 1653–1661.

Hettmann, K., Marks, M. A. W., Kreissig, K., Zack, T., Wenzel, T., Rekämper, M., Jacob, D. E. & Markl, G. (2014). The geochemistry of Tl and its isotopes during magmatic and hydrothermal processes: The peralkaline Ilímaussaq complex, southwest Greenland. *Chemical Geology* **366**, 1–13.

Karup-Møller, S. (1983). Lomonosovite from the Ilímaussaq intrusion, South Greenland. *Neues Jahrbuch für Mineralogie, Abhandlungen* **148**, 83–96.

Karup-Møller, S. (1986a). Murmanite from the Ilímaussaq alkaline complex, South Greenland. *Neues Jahrbuch für Mineralogie, Abhandlungen* **155**, 77–88.

Karup-Møller, S. (1986b). Epistolite from the Ilímaussaq alkaline complex in south Greenland. *Neues Jahrbuch für Mineralogie, Abhandlungen* **155**, 289–304.

Karup-Møller, S. & Rose-Hansen, J. (2013). New data on eudialyte decomposition minerals from kakortokites and associated pegmatites of the Ilímaussaq complex, South Greenland. *Bulletin of the Geological Society of Denmark* **61**, 47–70.

Karup-Møller, S., Rose-Hansen, J. & Sørensen, H. (2010). Eudialyte decomposition minerals with new hitherto undescribed phases from the Ilímaussaq complex, South Greenland. *Bulletin of the Geological Society of Denmark* **58**, 75–88.

Khomyakov, A. P. (1995). *Mineralogy of Hyperagpaitic Alkaline Rocks*. Oxford: Clarendon Press, 223 pp.

Khomyakov, A. P. & Sørensen, H. (2001). Zoning in steenstrupine-(Ce) from the Ilímaussaq alkaline complex, South Greenland: a review and discussion. In: Sørensen, H. (ed.) *The Ilímaussaq alkaline complex, South Greenland: status of mineralogical research with new results. Geology of Greenland Survey Bulletin* **190**, 109–118.

Khomyakov, A. P., Sørensen, H., Petersen, O. V. & Bailey, J. C. (2001). Naujakasite from the Ilímaussaq alkaline complex, South Greenland, and the Lovozero alkaline complex, Kola Peninsula, Russia: a comparison. In: Sørensen, H. (ed.) *The Ilímaussaq alkaline complex, South Greenland: status of mineralogical research with new results. Geology of Greenland Survey Bulletin* **190**, 95–108.

Khomyakov, A. P., Nechelyustov, G. N. & Rastsvetaeva, R. K. (2009). Voronkovite, $Na_{15}(Na,Ca,Ce)_3(Mn,Ca)_3Fe_3Zr_3Si_{26}O_{72}(OH,O)_4Cl{\cdot}H_2O$, a new mineral species of the eudialyte group from the Lovozero alkaline pluton, Kola Peninsula, Russia. *Geology of Ore Deposits* **51**, 750–756.

Kogarko, L. N. (1977). *Problems of the origin of agpaitic magmas*. Nauka (in Russian).

Konnerup-Madsen, J. (2001). A review of the composition and evolution of hydrocarbon gases during solidification of the Ilímaussaq alkaline complex, South Greenland. *Geology of Greenland Survey Bulletin* **190**, 159–166.

Krumrei, T. V., Villa, I. M., Marks, M. A. W. & Markl, G. (2006). A $^{40}Ar/^{39}Ar$ and U/Pb study of the Ilímaussaq complex, South Greenland: implication for ^{40}K decay constant and for the duration of magmatic activity in a peralkaline complex. *Chemical Geology* **227**, 258–273.

Krumrei, T. V., Pernicka, E., Kaliwoda, M. & Markl, G. (2007). Volatiles in a peralkaline system: Abiogenic hydrocarbons and F–Cl–Br systematics in the naujaite of the Ilímaussaq intrusion, South Greenland. *Lithos* **95**, 298–314.

Larsen, A. O. (ed.) (2010). *The Langesundsfjord. History, Geology, Pegmatites, Minerals*. Bode, 234 pp.

Larsen, L. M. (1976). Clinopyroxenes and coexisting mafic minerals from the alkaline Ilímaussaq intrusion, south Greenland. *Journal of Petrology* **17**, 258–290.

Larsen, L. M. & Steenfelt, A. (1974). Alkali loss and retention in an iron-rich peralkaline phonolitic dyke from the Gardar province, south Greenland. *Lithos* **7**, 81–90.

Macdonald, R., Karup-Møller, S. & Rose-Hansen, J. (2007). Astrophyllite-group minerals from the Ilímaussaq complex, South Greenland. *Mineralogical Magazine* **71**, 1–16.

Markl, G. & Baumgartner, L. (2002). pH changes in peralkaline late-magmatic fluids. *Contributions to Mineralogy and Petrology* **144**, 331–346.

Markl, G., Marks, M. A. W., Schwinn, G. & Sommer, H. (2001). Phase equilibrium constraints on intensive crystallization parameters of the Ilímaussaq Complex, South Greenland. *Journal of Petrology* **42**, 2231–2257.

Marks, M. A. W. & Markl, G. (2003). Ilímaussaq 'en miniature': closed-system fractionation in an agpaitic dyke rock from the Gardar Province, South Greenland. *Mineralogical Magazine* **67**, 893–919.

Marks, M. A. W. & Markl, G. (2015). The Ilímaussaq Alkaline Complex, South Greenland. In: Charlier, B., Namur, O., Latypov, R. & Tegner, C. (eds) *Layered Intrusions*. Springer, pp. 649–691.

Marks, M. A. W., Hettmann, K., Schilling, J., Frost, B. R. & Markl, G. (2011). The mineralogical diversity of alkaline igneous rocks: critical factors for the transition from miaskitic to agpaitic phase assemblages. *Journal of Petrology* **52**, 439–455.

Pekov, I. V., Krivovichev, S. V., Zolotarev, A. A., Yakovenchuk, V. N., Armbruster, T. & Pakhomovsky, Y. A. (2009). Crystal chemistry and nomenclature of the lovozerite group. *European Journal of Mineralogy* **21**, 1061–1071.

Petersen, O. V., Johnsen, O., Bernhardt, H.-J. & Medenbach, O. (1993). Dorfmanite, $Na_2HPO_4{\cdot}2H_2O$, from the Ilímaussaq alkaline complex, South Greenland. *Neues Jahrbuch für Mineralogie, Monatshefte* **1993**(**6**), 254–258.

Petersen, O. V., Khomyakov, A. P. & Sørensen, H. (2001). Natrophosphate from the Ilímaussaq alkaline complex, South Greenland. In: Sørensen, H. (ed.) *The Ilímaussaq alkaline complex, South Greenland: status of mineralogical research with new results. Geology of Greenland Survey Bulletin* **190**, 139–141.

Pfaff, K., Krumrei, T., Marks, M., Wenzel, T., Rudolf, T. & Markl, G. (2008). Chemical and physical evolution of the 'lower layered sequence' from the nepheline syenitic Ilímaussaq intrusion, South Greenland: Implications for the origin of magmatic layering in peralkaline felsic liquids. *Lithos* **106**, 280–296.

Piilonen, P., Lalonde, A. E., McDonald, A. M., Gault, R. A. & Larsen, A. O. (2003). Insights into astrophyllite-group minerals. I. Nomenclature, composition and development of a standardized general formula. *Canadian Mineralogist* **41**, 1–26.

Robles, E. R., Fontan, F., Monchoux, P., Sørensen, H. & de Parceval, P. (2001). Hiortdahlite II from the Ilímaussaq

alkaline complex, South Greenland, the Tamazeght complex, Morocco, and the Iles de Los, Guinea. In: Sørensen, H. (ed.) *The Ilímaussaq alkaline complex, South Greenland: status of mineralogical research with new results. Geology of Greenland Survey Bulletin* **190**, 131–137.

Rønsbo, J. G., Leonardsen, E. S., Petersen, O. V. & Jonsen, O. (1983). Second occurrence of vuonnemite: the Ilímaussaq alkaline intrusion, South West Greenland. *Neues Jahrbuch für Mineralogie, Monatshefte* **1983**, 451–460.

Rønsbo, J. G., Sørensen, H., Robles, E. R., Fontan, F. & Monchoux, P. (2014). Rinkite–nacareniobsite-(Ce) solid solution series and hainite from the Ilímaussaq alkaline complex: occurrence and compositional variation. *Bulletin of the Geological Society of Denmark* **62**, 1–15.

Rose-Hansen, J. & Sørensen, H. (2002). *Geology of the lujavrites from the Ilímaussaq alkaline complex, South Greenland, with information from seven bore holes. Meddelelser om Grønland, Geoscience* **40**, 58 pp.

Salvi, S., Fontan, F., Monchoux, P., Williams-Jones, A. E. & Moine, B. (2000). Hydrothermal mobilization of high field strength elements in alkaline igneous systems: evidence from the Tamazeght Complex (Morocco). *Economic Geology* **95**, 559–576.

Schilling, J., Marks, M., Wenzel, T. & Markl, G. (2009). Reconstruction of magmatic to subsolidus processes in an agpaitic system using eudialyte textures and composition: a case study from Tamazeght, Morocco. *Canadian Mineralogist* **47**, 351–365.

Sokolova, E. & Camara, F. (2008). From structure topology to chemical composition. VIII. Titanium silicates: the crystal chemistry of mosandrite from type locality of Låven (Skådön), Langesundsfjorden, Larvik, Vestfold, Norway. *Mineralogical Magazine* **72**, 887–897.

Sokolova, E. & Hawthorne, F. C. (2004). The crystal chemistry of epistolite. *Canadian Mineralogist* **42**, 797–806.

Sørensen, E. (1982). *Water-soluble substances in Kvanefjeld lujavrite. Report*. Risø National Laboratory, 4 pp.

Sørensen, H. (1962). *On the occurrence of steenstrupine in the Ilímaussaq massif, southwest Greenland. Meddelelser om Grønland* **167**(**1**), 251 pp.

Sørensen, H. (1974). *The Alkaline Rocks*. John Wiley, 621 pp.

Sørensen, H. (1992). Agpaitic nepheline syenite: a potential source of rare elements. *Applied Geochemistry* **7**, 417–427.

Sørensen, H. (1997). The agpaitic rocks—an overview. *Mineralogical Magazine* **61**, 485–498.

Sørensen, H. (2001). Brief introduction to the geology of the Ilímaussaq complex, South Greenland, and its exploration history. In: Sørensen, H. (ed.) *The Ilímaussaq alkaline complex, South Greenland: status of mineralogical research with new results. Geology of Greenland Survey Bulletin* **190**, 7–23.

Sørensen, H. (2006). *The Ilímaussaq alkaline complex, South Greenland—an overview of 200 years of research and an outlook. Meddelelser om Grønland, Geoscience* **45**, 70 pp.

Sørensen, H. & Larsen, L. M. (2001). The hyper-agpaitic stage in the evolution of the Ilímaussaq alkaline complex, South Greenland. In: Sørensen, H. (ed.) *The Ilímaussaq alkaline complex, South Greenland: status of mineralogical research with new results. Geology of Greenland Survey Bulletin* **190**, 83–94.

Sørensen, H., Leonardsen, E. S. & Petersen, O. V. (1970). Trona and thermonatrite from the Ilímaussaq alkaline intrusion, south Greenland. *Bulletin of the Geological Society of Denmark* **20**, 1–19.

Sørensen, H., Bailey, J. C. & Rose-Hansen, J. (2011). The emplacement and crystallization of the U–Th–REE-rich agpaitic and hyperagpaitic lujavrites at Kvanefjeld, Ilímaussaq alkaline complex, South Greenland. *Bulletin of the Geological Society of Denmark* **59**, 69–92.

Upton, B. G. J. (2014). *Tectono-magmatic evolution of the younger Gardar southern rift, South Greenland. Geological Survey of Denmark and Greenland Bulletin* **29**, 124 pp.

Ussing, N. V. (1912). Geology of the country around Julianehaab, Greenland. *Meddelelser om Grønland* **38**, 1–376.

Waight, T., Baker, J. & Willigers, B. (2002). Rb isotope dilution analyses by MC-ICPMS using Zr to correct for mass fractionation: towards improved Rb–Sr geochronology? *Chemical Geology* **186**, 99–116.

White, R. W., Powell, R. & Baldwin J. A. (2008). Calculated phase equilibria involving chemical potentials to investigate the textural evolution of metamorphic rocks. *Journal of Metamorphic Geology* **26**, 181–198.

Yakovenchuk, V. N., Ivanyuk, G. Yu., Pakhomovsky, Ya. A. & Men'shikov, Yu. P. (2005). *Khibiny*. Laplandia Minerals.

Zen, E-a. (1966). *Construction of pressure–temperature diagrams for multicomponent systems after the method of Schreinemakers—a geometric approach. US Geological Survey Bulletin* **1225**, 56 pp.